Charm contribution to neutrino-induced production of opposite-sign dimuons*

Choy-Heng Lai
Fermi National Accelerator Laboratory,† Batavia, Illinois 60510
and Department of Physics, The University of Chicago, Chicago, Illinois 60637
(Received 6 April 1978)

A systematic study of the charm contribution to the neutrino-induced opposite-sign dimuon events is presented. Theoretical predictions, taking into account the threshold effects, the experimental cuts and the beam spectrum, are compared with the CERN-Dortmund-Heidelberg-Saclay data. The behavior of the charmed-quark fragmentation function is also investigated.

I. INTRODUCTION

Neutrino- and antineutrino-induced events with two muons in the final state were reported by two experimental groups[1,2] at Fermilab two years ago. Since then, μe events have also been observed in bubble chambers operating at Fermilab[3] and CERN,[4] and recently the CERN-Dortmund-Heidelberg-Saclay (CDHS) group has also reported their first results on opposite-sign dimuon events.[5] While it is generally believed that the excitation of charm and its subsequent semileptonic decay would lead to such signals,[6] it is not entirely clear yet whether additional particles with other new quantum numbers are required to explain these observations. Indeed, the so-called high-y anomaly[7] and the rise in $\sigma^{\bar{\nu}}/\sigma^{\nu}$ (Ref. 8) observed by the Fermilab-Harvard-Pennsylvania-Rutgers-Wisconsin (FHPRW) group seemed to indicate new quark degrees of freedom and even possibly new couplings of antineutrinos to hadrons. Some earlier suggestions that $SU(2)\times U(1)$ gauge models containing right-handed currents provided a natural mechanism for enhancing the antineutrino y distributions at high y were made by De Rújula *et al.*[9] and Barnett,[9] and a detailed study of possible right-handed quark transitions in inclusive charged-current antineutrino reactions within the context of several gauge models has been recently given by Albright and Shrock.[9]

The recent CDHS,[10] and CalTech-Fermilab-Rockefeller (CFR) (Ref. 11) and BEBC (Ref. 12) results, however, do not confirm the FHPRW observations. No evidence for the anomalous sharp rise in the ratio of antineutrino-to-neutrino charged-current cross sections $\sigma^{\bar{\nu}}/\sigma^{\nu}$ is seen by the CDHS and CFR experiments, and the BEBC results, while not inconsistent with a slow increase with energy, do not reproduce the FHPRW data, and any increase of $\sigma^{\bar{\nu}}/\sigma^{\nu}$ with energy seems due more to a decrease in σ^{ν}/E than to an increase in $\sigma^{\bar{\nu}}/E$. Also, the CDHS antineutrino data on the average y values, as well as the $B_{\bar{\nu}}$ parameter

$$B_{\bar{\nu}} \equiv -\int xF_3^{\bar{\nu}}(x)dx \Big/ \int F_2^{\bar{\nu}}(x)dx$$

show no sign of energy-dependent effects, although the world data on B_{ν} without CDHS indicates a mild but statistically significant energy dependence.[13]

Motivated in part by the recent CDHS results, we present here a systematic study of the charm contribution to opposite-sign dimuon production by neutrinos. The purpose is to ascertain the extent to which the charm production and subsequent decay picture is able to explain the dimuon events, so that any new physical effects, such as additional new hadronic states carrying new quantum numbers and new leptons, can be separated from the charm background. We take into account in our study the threshold effects[14] inherent in such heavy-particle production processes, as well as the experimental cuts and incident neutrino spectrum. The quark-parton-model language is used, and theoretical predictions based on the standard Glashow-Iliopoulos-Maiani (GIM) (Ref. 15) extended Weinberg-Salem[16] model are compared with available data from the CDHS experiment, which at present has the most statistics.

We begin in Sec. II by describing the model for dilepton production and the calculations. A discussion is given in Sec. III on the choice of the quark fragmentation function and the phenomenological consequences. The detailed results are presented in Sec. IV with cuts and flux-averaging appropriate for the CDHS experiment. Section V contains some conclusions of our study.

II. MODEL FOR DILEPTON PRODUCTION

We consider here the neutrino and antineutrino reactions

$$\nu_{\mu}(\bar{\nu}_{\mu}) + T \to \mu^{\mp} l^{\pm} + X , \tag{1}$$

where T is the target hadron, and l is either a muon or an electron. Owing to the fact that the

total interaction cross section for (anti) neutrinos is small, experimental data with reasonable statistics come mainly from experiments with heavy isoscalar targets. Consequently, we shall concentrate on reactions in which T is an isoscalar, and investigate in this work whether reaction (1) can be interpreted as resutling from the sequence of reactions

$$\nu_\mu(\bar{\nu}_\mu)+T\to\mu^{\mp}+C+X \qquad C\to l^{\pm}+\nu(\bar{\nu})+X' \tag{2}$$

where C is a charmed particle.

Our quark-parton-model calculation for the processes in (2) will be divided three parts, corresponding to the processes of charm excitation, the production of a charmed hadron by charmed-quark fragmentation, and the semileptonic decay of the charmed hadron C.

A. Charm excitation

Within the context of the GIM-Weinberg-Salam model, charm excitation by (anti)neutrinos can occur in several ways: For example,

(i) diffractive production of a charmed vector meson[17]

$$\nu_\mu(\bar{\nu}_\mu)+N\to\mu^-(\mu^+)+C^{*\pm}+X, \tag{3}$$

(ii) direct light-quark-to-charmed-quark transition

$$\nu_\mu+d\to\mu^-+c, \tag{4a}$$

$$\nu_\mu+s\to\mu^-+c, \tag{4b}$$

$$\bar{\nu}_\mu+\bar{d}\to\mu^++\bar{c}, \tag{4c}$$

$$\bar{\nu}_\mu+\bar{s}\to\mu^++\bar{c}, \tag{4d}$$

and

(iii) associated charm production

$$\nu_\mu(\bar{\nu}_\mu)+N\to\mu^-(\mu^+)+C^++C^-+X. \tag{5}$$

The diffractive production of charm [Fig. 1(a)] is somewhat outside the spirit of the quark-parton model, and the characteristics of the dilepton events from this source seem to disagree with experimental data: The vector meson C^* tends to emerge with most of the hadronic energy due to the diffractive cutoff in momentum transfer; thus the visible hadronic energy in such a process comes mainly from C^* decay, peaking at small energies. The experimental data on dilepton events do not show such a characteristic.

The associated-production process [Fig. 1(c)] necessarily has a higher threshold than for single-charm production, but nonetheless should contribute to the dilepton events (especially those of the same sign[18]). However, since the secondary

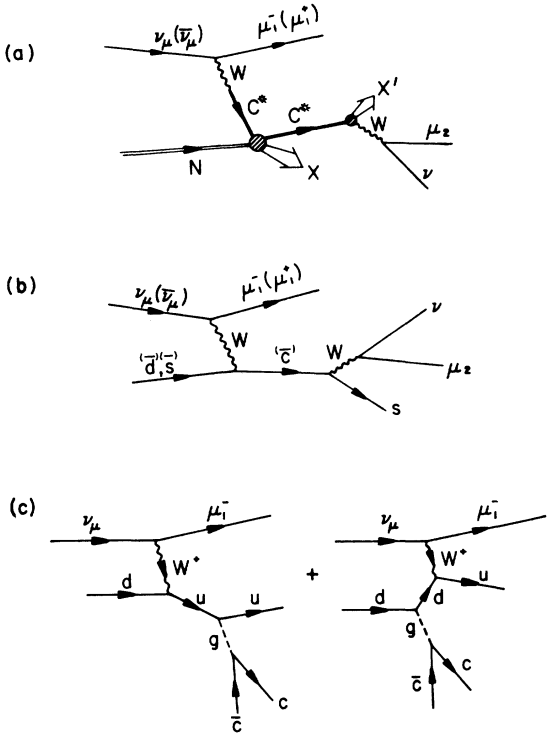

FIG. 1. (a) Diffractive production of a charmed vector meson C^* and subsequent semileptonic decay. (b) Light-quark-to-charmed-quark transition and subsequent $c\to s\mu\nu$ decay. (c) Neutrino-induced associated production of charm in QCD. The dotted lines denote colored gluons.

lepton can come from the decay of either of the charmed hadrons, this mechanism predicts that

$$\sigma^{\nu}(l^+l^-)=\sigma^{\nu}(l^-l^-),$$

$$\sigma^{\bar{\nu}}(l^+l^-)=\sigma^{\bar{\nu}}(l^+l^+).$$

Experimentally, same-sign dimuon events are observed only at rate of approximately 15–20% of that of opposite-sign dimuon events.[19] Thus the bulk of the opposite-sign dimuon events observed cannot be accounted for by the associated production of charm. A recent calculation[20] of the cross section for the inclusive neutrino production of charm-anticharm pairs within the framework of quantum chromodynamics (QCD) indicates a rate too small even to account for the same-sign dimuon events.

We believe that the deep-inelastic light-quark-to-charmed-quark transition picture [Fig. 1(b)] is a much more reasonable candidate for the major source of dilepton events. Our efforts here will thus be concentrated on this mode of charm excitation. Reactions (4a) and (4b) are expected to have roughly the same contribution since, while

reaction (4a) is Cabibbo-suppressed, the strange-quark content in the nucleon has been shown to be small experimentally. The same statement cannot be made for the antineutrino case [(4c) and (4d)]: both $\bar{d}$ and $\bar{s}$ contents, apart from small variations in parton-distribution parametrizations, are small.

The differential cross section for the inclusive production of charm can be written in the form[21]

$$\frac{d\sigma^{\nu,\bar{\nu}}}{dxdy}(c) = \frac{G^2 M_N E}{\pi}\left[xy^2 F_1^{\nu,\bar{\nu}} + (1-y)F_2^{\nu,\bar{\nu}} \mp y\left(1-\frac{y}{2}\right)xF_3^{\nu,\bar{\nu}}\right]. \quad (6)$$

where x and y are the usual scaling variables

$$x \equiv \frac{Q^2}{2M_N\nu}, \quad y \equiv \frac{\nu}{E} \quad (7)$$

$-Q^2 = q^2$ is the momentum transfer squared, E (E') is the energy of the incident (scattered) lepton, and $\nu \equiv (E - E')$ is the energy transfer, in the laboratory frame.

In Eq. (6), $F_2^{\nu,\bar{\nu}}$ and $F_1^{\nu,\bar{\nu}}$ are the weak analogs of the electric and magnetic structure functions, and F_3 in a parity-violating intereference term which contriubtes with opposite magnitude for neutrinos and antineutrinos. Bjorken scaling (as observed at intermediate energies) implies that these structure functions are dependent upon the variable x only, and several relations[21] have been established experimentally (at least approximately) between them:

(i) Callan-Gross relation[22]

$$2xF_1(x) = F_2(x), \quad (8a)$$

(ii) Maximal V-A interference

$$-2F_1(x) \simeq F_3(x). \quad (8b)$$

Using these relations, the inclusive differential cross section for charm production can be written in the simple form

$$\frac{d\sigma^{\nu,\bar{\nu}}}{dxdy}(c) = \frac{G^2 M_N E}{\pi} F_2^{\nu,\bar{\nu}}(x). \quad (9)$$

This is because, assuming left-handed currents only, the y dependence in such charged-current processes is determined by whether the neutrino (antineutrino) scatters off a quark or an antiquark (Table I).

In the quark-parton model, where the differential cross section is just given by an incoherent sum over current-parton scattering cross sections, the structure function F_2 is given by (for charmed-quark excitation only)

$$F_2^{\nu}(x) = 2x[\sin^2\theta_C d_N(x) + \cos^2\theta_C s_N(x)], \quad (10a)$$

TABLE I. y dependence in (anti)neutrino-(anti)quark scattering.

	$q \to q'$	$\bar{q} \to \bar{q}'$
ν	1	$(1-y)^2$
$\bar{\nu}$	$(1-y)^2$	1

$$F_2^{\bar{\nu}}(x) = 2x[\sin^2\theta_C \bar{d}_N(x) + \cos^2\theta_C \bar{s}_N(x)], \quad (10b)$$

where $q_N(x)[\bar{q}_N(x)]$ is just the probability of finding a quark (antiquark) of flavor q with momentum fraction x within the isoscalar nucleon.

An additional complication arises, however, in these light (d, s) quark to heavy quark transitions. It has been pointed out by several authors[14] that in this case, the structure functions F^{ν} are no longer scaling functions of x. Instead, taking into account the mass correction, the effective scaling variable takes the form

$$\xi_j = x + \frac{m_j^2}{2M_N E y}, \quad (11)$$

where m_j is the effective mass of the heavy quark q_j. Physically, the range of the variable ξ_j is restricted by the fact that in such heavy-quark production processes, the invariant mass W recoiling against the scattered lepton must satisfy

$$W > W_{\text{th}}, \quad W_{\text{th}} = \text{some threshold value}.$$

In terms of x and y, this means i.e.

$$y(1-x) \geq \frac{W_{\text{th}}^2 - M_N^2}{2M_N E},$$

i.e.,

$$E \geq \frac{W_{\text{th}}^2 - M_N^2}{2M_N}, \quad y \geq \frac{W_{\text{th}}^2 - M_N^2}{2M_N E}$$

$$x \geq 1 - \frac{W_{\text{th}}^2 - M_N^2}{2M_N E y}. \quad (12)$$

Taking the above into account, and generalizing Eq. (8) with x replaced by ξ_c, we then have the inclusive charm-production cross section (assuming left-handed transitions only)

$$\frac{d\sigma^{\nu,\bar{\nu}}}{dxdy}(c) = \frac{G^2 M_N E}{\pi}\left[1 - y\frac{xy^2}{2\xi_c} + \frac{xy}{\xi_c}\left(1-\tfrac{1}{2}y\right)\right] \times F_2^{\nu,\bar{\nu}}(\xi_c)\,\theta(W - W_c), \quad (13)$$

with

$$\xi_c = x + \frac{m_c^2}{2M_N E y}$$

and $F_2^{\nu,\bar{\nu}}$ given by Eqs. (10a) and (10b). For our calculations here, W_c has been taken to be

$$W_c = m_c + M_N,$$

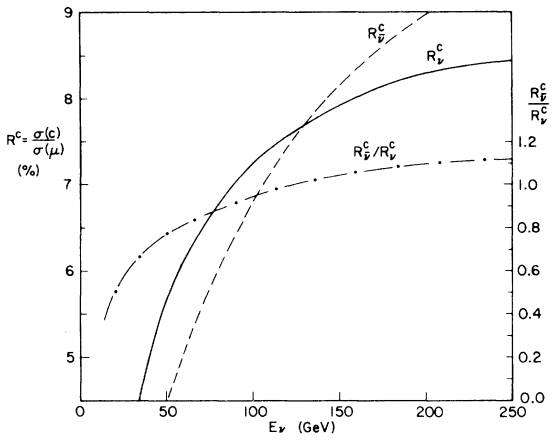

FIG. 2. Charm-production cross section, relative to single-muon charged-current (noncharm) cross section, as a function of incident neutrino energy.

with $m_c = 1.5$ GeV/c^2.

In Fig. 2 we have plotted the cross-section ratios $R^c_{\nu,\bar\nu}$ as a function of the incident (anti) neutrino energy, where

$$R^c_\nu = \frac{\sigma(\nu + d, s \to \mu^- + c)}{\sigma_{\text{noncharm}}(\bar\nu \to \mu^-)} ,$$

$$R^c_{\bar\nu} = \frac{\sigma(\bar\nu + \bar d, \bar s \to \mu^+ + \bar c)}{\sigma_{\text{noncharm}}(\bar\nu \to \mu^+)} .$$

Both rise steeply above threshold and level off at high energies. Over the energy range of ~50–250 GeV, the charm-production cross section is typically 5–10% of the single-muon charged-current cross section. A rough estimate of the dimuon cross section is then

$$\frac{\sigma(2\mu)}{\sigma(\mu)} \sim R^c B(C \to \mu\nu X) \sim (0.2\text{–}2) \times 10^{-2}$$

for a branching ratio of ~5–20%. This is slightly higher than the experimentally observed rate, but seems reasonable considering the fact that the experimental cuts have been ignored in the above estimate. We shall also see (in Sec. III) that the cross-section ratio in realistic experimental situations is actually quite sensitive to the choice of the quark fragmentation function.

We note that in this picture of charm excitation, we expect the following:

(i) *Very similar* characteristics for neutrinos and for antineutrino interactions (except for the x distributions to be discussed below)–in particular, a flat y distribution, with a threshold at small y, is predicted for both neutrinos and antineutrinos. (The distortion due to threshold effects and experimental cuts, however, especially for dimuon production, will be quite severe.)

(ii) The x distribution for antineutrino interactions is concentrated at small x, as expected for charm production off sea quarks, whereas the neutrino x distribution has, in addition, a rather strong valence-quark component.

(iii) The small x component, which reflects primarily the sea $s\bar s$ content and is present in both neutrino and antineutrino interactions, leads to predominantly $S = \pm 1$, $C = \pm 1$ final states. In contrast, $S = 0$, $C = +1$ final states, arising from valence strength $d \to c$ transitions, should only be observed in neutrino interactions.

Thus the two-component nature of the charm excitation, as manifested in the x distributions, is most important in verifying our present interpretation of the origin of the dilepton events. Furthermore, any significant difference between the other observed neutrino and antineutrino distributions would then be an indication of new couplings of antineutrinos or neutrinos to hadrons and/or additional quark (or lepton) degrees of freedom.

B. Charmed-hadron production

It is here assumed that when a heavy quark (in this case, charm) is produced in the collision of the incident (anti) neutrino with a quark constituent of the nucleon (as described by the differential cross section given in subsection A), it moves away from the other quarks with high momentum $\vec P$, and subsequently fragments into a cascade of hadrons with small transverse momentum with respect to $\vec P$ (Fig. 3). The new heavy hadron C appears as one of the fragments. The fragmentation of a quark q into a hadron H_q is usually described by a phenomenological function[23] (called the quark decay or fragmentation function)

$$D_{q|H_q}(z) ,$$

where z is the energy fraction carried by the hadron H_q.

In general,

$$\langle n(H_q)\rangle \equiv \int_{z_{\min}}^{1} D_{q|H_q}(z)\, dz$$

is the mean multiplicity of particles of type H_q emerging from the parent quark with $z > z_{\min}$.

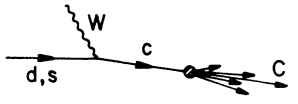

FIG. 3. Charmed-quark fragmentation into a charmed hadron C and other physical hadrons.

So far, the only fragmentation functions known are those of ordinary quarks (u, d, and s). Relatively little is known, both theoretically and experimentally, about how a charmed (or any heavy) quark fragments into a new hadron in the present energy regime. Presumably the question of mass corrections would come up again here. One purpose of our study is to investigate the sensitivity of our predictions to variations in these unknown functions. We have, in our calculations, used a number of parametrizations of $D(z)$. A discussion of the phenomenological consequences of the behavior of $D(z)$, especially as $z \to 1$, will be given later.

We thus write the differential cross section for charmed-hadron production in the following form:

$$\frac{d\sigma^{\nu,\bar{\nu}}}{dxdydz}(C) = \frac{d\sigma^{\nu,\bar{\nu}}}{dxdy}(c) D_{c|C}(z), \tag{14}$$

where $(d\sigma^{\nu,\bar{\nu}})/(dxdy)(c)$ is given by Eq. (13).

C. Weak semileptonic decay of the charmed hadron

Considered in the quark-parton model, the charmed hadron may decay semileptonically through the following processes:

$$c \to s + l^+ + \nu_l \sim \cos^2\theta_C,$$
$$c \to d + l^+ + \nu_l \sim \sin^2\theta_C,$$
$$\bar{c} \to \bar{s} + l^- + \bar{\nu}_l \sim \cos^2\theta_C,$$
$$\bar{c} \to \bar{d} + l^- + \bar{\nu}_l \sim \sin^2\theta_C,$$

where θ_C is the Cabibbo angle. Because of the Cabibbo suppression, we shall consider only $c \to s$ $(c \to s)$ decay and set $\cos^2\theta_C = 1$. The charged-lepton spectrum in the laboratory frame is then simply

$$H(E_l, \zeta) \equiv \frac{1}{\Gamma}\frac{d\Gamma}{dE_l d\zeta} = N \frac{(Q^2 - m_s^2)^2 (m_c^2 - Q^2)}{Q^2} E_l dE_l d\zeta,$$

where N is a normalization factor, Q^2 the momentum transfer squared, $\zeta = \frac{1}{2}(\cos\theta + 1)$, and θ is the angle between the charged lepton and the quark (hadron) momenta.

This completes our descritpion of the dilepton production process, and the differential cross section can be written in the compact form

$$d\sigma^{\nu,\bar{\nu}}(\mu l) = \frac{d\sigma^{\nu,\bar{\nu}}}{dxdy}(c) D_{c|C}(z) B_l H(E_l, \zeta) dxdydzdE_l d\zeta, \tag{15}$$

where B_l is the semileptonic branching ratio for C.

It should be noted that we have not in our calculations taken into account the transverse-momentum spread p_T in the quark fragmentation process. This is, of course, particularly relevant in the resutling k_T distribution of the secondary lepton [where k_T is the momentum out of the production plane,

$$k_T = \vec{k}_l \cdot (\vec{k}_\nu \times \vec{k}_\mu)/(|\vec{k}_\nu| \cdot |\vec{k}_\mu|)].$$

Generally, an exponential function, e^{-bp_T} is used with b appropriately adjusted to give a reasonable value of $\langle p_T \rangle$. There is also the question of whether the parton picture correctly describes the decay mechanism. The decays $D \to Kl\nu$, $D \to K^* l\nu$ have been used by some authors.[24] Our feeling is that with our present knowledge of the weak-decay properties of the charmed hadrons, and the fact that other charmed hadrons (D^*, e.g.) could also have been produced, the parton calculation should provide an equally adequate description of the decay process.

In our calculations, we have used the Field-Feynman[25] (FF) parametrization of the quark-parton distributions, which includes a sea contribution

$$u_{\text{sea}}(\xi) = \bar{u}_{\text{sea}}(\xi) = 0.17\,\xi^{-1}(1-\xi)^{10},$$
$$d_{\text{sea}}(\xi) = \bar{d}_{\text{sea}}(\xi) = 0.17\,\xi^{-1}(1-\xi)^{7},$$
$$s_{\text{sea}}(\xi) = \bar{s}_{\text{sea}}(\xi) = 0.10\,\xi^{-1}(1-\xi)^{8}.$$

For comparison, we have also used the parametrization by Pakvasa-Parashar-Tuan[26] (PPT), which has an SU(3) symmetric sea characterized by a less rapid decrease with ξ,

$$s(\xi) = \bar{s}(\xi) = \bar{u}(\xi) = \bar{d}(\xi) = 0.1\,\xi^{-1}(1-\xi)^{7/2}.$$

We have found that most distributions are not sensitively dependent upon the parton-distribution parametrization. The dimuon production rate is somewhat enhanced in the PPT parametrization as can be expected,

$$\frac{\sigma^{\nu}(\mu\mu)_{\text{FF}}}{\sigma^{\nu}(\mu\mu)_{\text{PPT}}} \sim 0.7.$$

It should perhaps be noted that some recent determinations of the quark-parton distributions favor a sea-quark distribution that falls more steeply as $x \to 1$ than the PPT parametrization. Duke and Taylor[27] obtain a proton sea-quark distribution

$$x\bar{u}_p(x) = x\bar{d}_p(x) = 1.2(1-x)^{8},$$
$$x\bar{s}_p(x) = xs_p(x) = 0.135(1-x)^{5.75},$$

from single-particle inclusive reactions, which also give good agreement with the experimental production cross section for low-mass muon pairs

by the Drell-Yan process. (The enhanced $\bar{u}$ and $\bar{d}$ distributions are interpreted as due to the significant contribution of the conversion of gluons to quark-antiquark pairs in the initial hadron collision.) A combined analysis[28] of the reactions $pN \to l^+l^- X$ (in the low-mass region) and $eN \to eX$ also suggests a sea-quark distribution of the form

$$x\bar{u}_p(x) = x\bar{d}_p(x) = xs_p(x) = 0.145(1-x)^{11}(1+10x).$$

Finally, an experimental study of the high-mass dimuon continuum in proton-nucleus collisions,[29] when compared with the Drell-Yan annihilation model, also yields a sea quark distribution

$$x\bar{u}_p(x) = x\bar{d}_p(x) = xd_p(x) = x\bar{s}_p(x) = 0.6(1-x)^{10}$$

In all of these cases, either isospin ($\bar{u} = \bar{d}$) or SU(3) ($\bar{u} = \bar{d} = \bar{s}$) symmetry is assumed. The FF parametrization, with its flavor-asymmetric sea, is not in striking disagreement with these determinations, and until more detailed information on the different antiquark and strange-quark distributions is available, it should be a reasonable form to use in these calculations.

III. QUARK-DECAY-FUNCTION PARAMETRIZATION

As mentioned earlier, the form of the quark decay function $D(z)$ remains a theoretical assumption in our calculations. A recent parametrization of $D(z)$ (for ordinary quarks), determined from particle distributions in lepton-hadron and e^+e^- interactions and supplemented by theoretical arguments, was given by Field and Feynman.[25] Their $D_{u|\pi^+}(z)$ [which can be taken to be equal to $D_{c|D^+}(z)$ in exact SU(4)] turns out to be similar to the form $z^{-1}(1-z)$ suggested by Sehgal and Zerwas[6](SZ). Both behave as z^{-1} as $z \to 0$, while

$$\left.\begin{aligned} D^{FF}(z) &\sim \text{constant} \\ D^{SZ}(z) &\sim (1-z) \end{aligned}\right\} z \to 1 .$$

Other forms of $D(z)$ have also been suggested, e.g.,

z^{-1} (Seiden[30])

e^{-3z} (Barger-Gottschalk-Phillips[31])

$(1-z)^2$ (Gronau–Llewellyn Smith–Walsh–Wolfram–Yang[32]).

All these forms of $D(z)$ favor the small z region, with varying degrees of large z contributions. The FF and SZ as well as the z^{-1} forms, in particular, give rise to a logarithmic increase in particle multiplicity as energy increases (this seems to fit the leptoproduction of π's reasonably well). These parametrizations, however, are likely to be asymptotic forms, appropriate when the quark and hadron masses are completely negligible compared to the fragmenting quark energy. For the fragmentation of the charmed quark (or any heavy quark) into new hadrons, significantly different behavior may prevail in the present energy regime. It is not even clear whether the fragmentation function should scale in this case.

Recently, some attempts have been made to suggest a behavior for the charmed-quark fragmentation function, quite different from that of the ordinary quarks:

(i) Suzuki[33] proposes a model in which the produced quark decelerates by converting its kinetic energy into physical hadrons and becomes a fireball with mass

$$M_q = m_q + Q ,$$

where m_q is the quark mass and Q is a parameter assumed to be independent of flavor. In the rest frame of the fireball, the energy distribution of the physical hadrons obeys the Boltzman distribution, and in the laboratory frame, the fragmentation function takes the form

$$D(z) = C' \exp\left[-\tfrac{1}{2}\kappa M_q \left(z + \frac{m_h^2}{m_q^2}\frac{1}{z}\right)\right],$$

which has a maximum at $z = m_h/(m_q+Q)$, falling rapidly for $m_h^2/m_q^2 \ll 1$ as $z \to 0$ and 1. For qualitative arguments, this function can be taken to be

$$D(z) \sim \delta\left(z - \frac{m_D}{m_c+Q}\right) = \delta(z-0.75)$$

for $m_D = 1.87$, $m_c = 1.5$, and $Q = 1.0$ GeV.

(ii) This strong peaking at high z is also suggested by Bjorken[34] with the following qualitative argument: When the heavy quark is produced, with energy transfer $\nu \gg m_q$, it moves away from the target with energy E_q and high velocity and hence large $\gamma_q = E_q/m_q$. *Asymptotically* then hadrons produced in the fragmentation process will have γ values $\gamma_h \sim \gamma_q$; consequently

$$\frac{E_H}{E_h} = \frac{m_H}{m_h} \times \frac{E_H/m_H}{E_h/m_h} \sim \frac{m_H}{m_h} ,$$

where H is the hadron containing the heavy quark. In the case where $m_H \gg m_h$, we see that the heavy hadron H tends to retain much of the original quark energy.

(iii) Assuming the validity of the "reciprocity relation"[35] at $z \sim 1$:

$$D_{q|H}(z) = f_H^q(z)$$

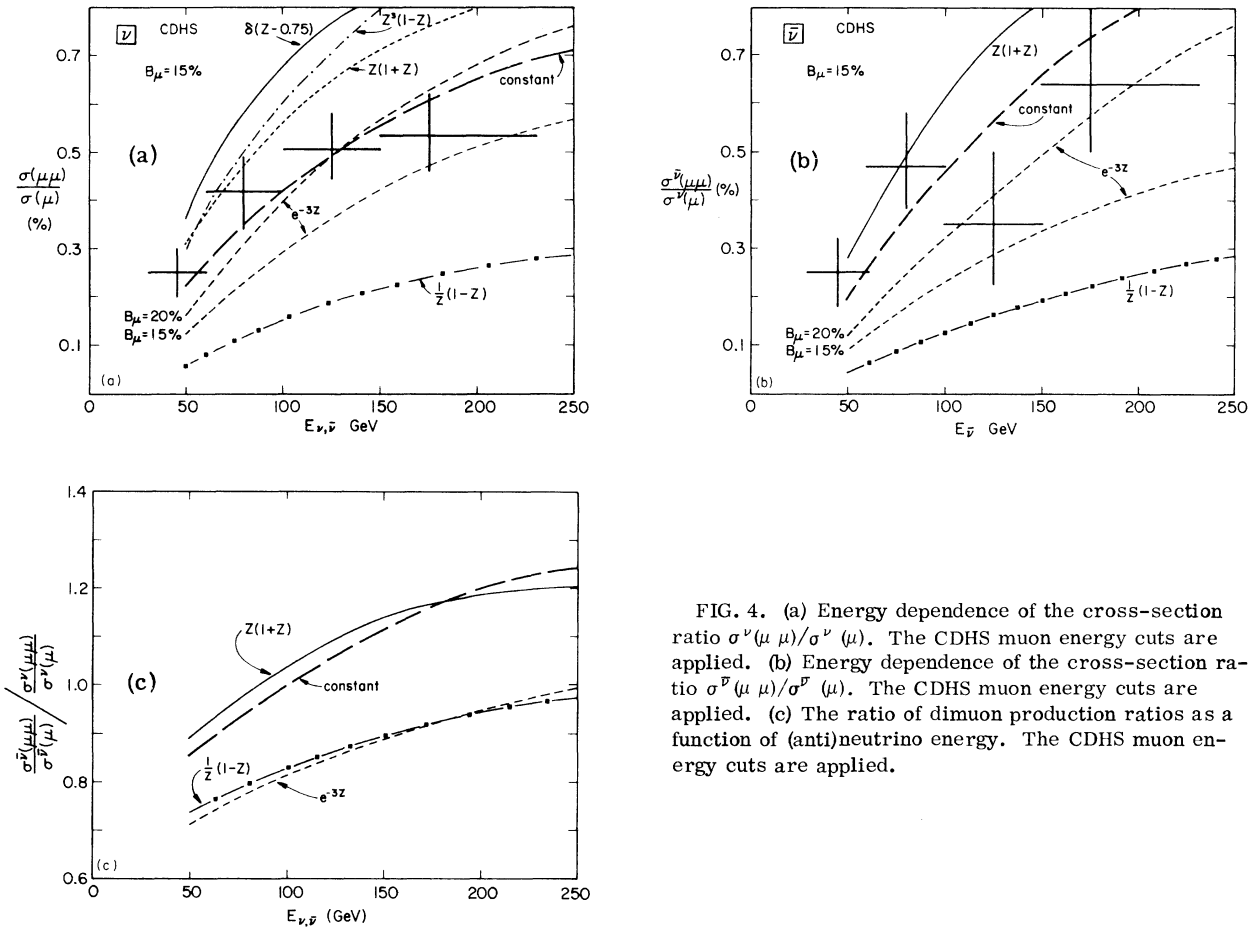

FIG. 4. (a) Energy dependence of the cross-section ratio $\sigma^{\nu}(\mu\,\mu)/\sigma^{\nu}(\mu)$. The CDHS muon energy cuts are applied. (b) Energy dependence of the cross-section ratio $\sigma^{\bar{\nu}}(\mu\,\mu)/\sigma^{\bar{\nu}}(\mu)$. The CDHS muon energy cuts are applied. (c) The ratio of dimuon production ratios as a function of (anti)neutrino energy. The CDHS muon energy cuts are applied.

where $f_H^q(z)$ is the q-type quark density in the hadron H, Kartvelishvili *et al.*[36] have arrived at a charmed-quark fragmentation of the form

$$D(z) \sim z^3(1-z)$$

which peaks at $z = 0.7$–0.8. Note that $D(z)$ vanishes both as $z \to 0$ and $z \to 1$.

We have investigated the sensitivity of the various characteristics of the dimuon events to the choice of the quark fragmentation functions. We assume that only one charmed hadron is produced in each dimuon event and normalize the fragmentation functions so that

$$\int_{z_{\min}}^{1} D(z)dz = 1\,,$$

where $z_{\min} = m_c/\nu$. First we calculate the cross-section ratio $\sigma(\mu\mu)/\sigma(\mu)$ as a function of the incident neutrino energy, folding in the energy cut on the detected muons, for the various fragmentation functions. These are plotted in Fig. 4, assuming a semileptonic branching ratio of 15%. The form $(1/z)(1-z)$ gives a cross-section ratio far below the CDHS data points, even when the $D \to K\mu\nu$ decay matrix element is used. [The effect of the slight phase space difference between the $D \to K\mu\nu$ and $c \to s\mu\nu$ decay is most significant for fragmentation functions favoring small z, a factor of $\lesssim 2$ in the case of $(1/z)(1-z)$.] Fragmentation functions favoring high z values, $\delta(z-0.75)$, $z(1+z)$, $z^3(1-z)$, all give rather large values for the cross-section ratio, especially at high energies ($E_\nu \gtrsim 100$ GeV). The best fit seems to be that given by $D(z) = \text{constant}$, although the forms e^{-3z}, with a slightly larger branching ratio of 20% (to perhaps correct for the slight underestimate in the $c \to s\mu\nu$ decay) and $z(1+z)$ with $B_\mu \simeq 10\%$ are also not far off.

Figure 4(c) shows the energy dependence of the ratio

$$R_\tau \equiv \frac{\sigma^{\bar{\nu}}(\mu\mu)}{\sigma^{\bar{\nu}}(\mu)} \Big/ \frac{\sigma^{\nu}(\mu\mu)}{\sigma^{\nu}(\mu)}\,.$$

Here the semileptonic branching ratio of charm cancels out, and the relative neutrino and antineutrino normalizations do not enter. It has been

pointed by Barnett and Martin[37] that this ratio is a rather sensitive test for the existence of a right-handed current of the type $(u,b)_R$ (where b is a heavy quark of charge $-\frac{1}{3}$ and mass m_b ~4–7 GeV) with R_ν rising sharply above threshold to a value of ~2–6 (depending on m_b) at $E \sim 150$ GeV. Asymptotic-freedom corrections, however, are quite important in this case. The CDHS data points, while not precise enough to differentiate between the different fragmentation functions, do seem to exclude a b quark with $m_b < 8$–9 GeV unless the semileptonic branching of the b quark is extremely small.[37]

For other experimental characteristics of the dimuon events, our study seems to indicate that while we can expect the average values as well as the distributions of the various quantities related with the hadronic vertex and charmed hadron decay to be reflective of the choice of $D(z)$, some overall quantities of the process are also affected. In particular, a $D(z)$ with substantial values as $z \to 1$ means that the charmed hadron is likely to emerge with a large fraction of the momentum and energy transferred. Thus its decay would, on the average, lead to more energetic $\mu(e)$ and ν in the final state. Since in most experiments the incident (anti) neutrino energy is not known, $E_{\rm vis}$ $(=E_{\rm Had}+E_{\mu_1}+E_l)$ in such cases will be substantially less than E_ν. It is then clear that the experimentally determined quantities

$$\nu_{\rm vis} = (E_{\rm vis} - E_{\mu_1}),$$

$$Q_{\rm vis}^2 = 2E_{\rm vis}E_{\mu_1}(1-\cos\theta_{\mu_1}),$$

$$x_{\rm vis} = Q_{\rm vis}^2/(2M_N E_{\rm vis}),$$

$$y_{\rm vis} = \nu_{\rm vis}/E_{\rm vis},$$

take on very different values.

In Table II we list the average values of the various experimental observables, obtained using the various forms of $D(z)$, for the CDHS experiment. The average values of E_{μ_2}, $\langle E_{\mu_1}\rangle/\langle E_{\mu_2}\rangle$, $\Delta\phi$, $z_{\mu_2} = E_{\mu_2}/(E_{\mu_2}+E_{\rm had})$, $\gamma = (E_{\mu_1}-E_{\mu_2})/(E_{\mu_1}+E_{\mu_2})$ seem to be particularly sensitive to the form of $D(z)$. The distributions of these quantities also show sizable effects: The E_{μ_2} spectrum (Fig. 6) has a longer tail at high energies, the β $(=E_{\mu_2}/E_{\mu_1})$ distribution (Fig. 7) has a tail extending way beyond 2, the z_{μ_2} distribution (Fig. 19) broadens, the $\Delta\phi$ distribution (Fig. 13) becomes more sharply peaked at 180°, and the large-positive-γ region (Fig. 9) is less enhanced, when the high-z end of the fragmentation function becomes more emphasized. A fuller discussion on the distributions is given in Sec. IV. But from the average values in Table II alone, there seems to be a slight favor for the fragmentation functions $D(z) \sim e^{-3z}$ and constant.

Perhaps we should add that, since the incident neutrino energy in the CDHS experiment is known to some accuracy, the average value of the ratio $E_{\rm vis}/E_\nu$ can place a severe constraint on the possible behavior of the charmed-quark fragmentation function. This sensitivity, however, may not be so clear cut: A $D(z)$ which sharply peaks at $z=1$

TABLE II. Average values of experimental quantities of the CDHS experiment.

	$\frac{1}{z}(1-z)$	e^{-3z}	const	$z^3(1-z)$	$z(1+z)$	$\delta(z-0.75)$	Data [a]
$E_{\rm vis}$ (±5 GeV)	129	128	120	118	117	108	108 ±3
E_{μ_1} (GeV)	47.0	48.0	49.0	50.0	50.5	49.5	45 ±2
E_{μ_2} (GeV)	11.0	12.7	15.6	16.4	17.5	16.5	13.7 ±1.0
$x_{\rm vis}$	0.20	0.20	0.21	0.21	0.22	0.22	0.24 ±0.01
$y_{\rm vis}$	0.65	0.63	0.60	0.59	0.57	0.56	0.58 ±0.02
$E_{\rm vis}/E_\nu$ (ν_K only)	0.94	0.93	0.87	0.86	0.85	0.79	0.92 ±0.04
$\frac{\langle E_{\mu_1}\rangle}{\langle E_{\mu_2}\rangle}$	4.27	3.78	3.14	3.05	2.89	3.00	3.28 ±0.39
$\Delta\phi$ [b]	124°	126°	130°	134°	136°	141°	128° ±3°
$\frac{E_{\mu_2}}{E_{\mu_2}+E_{\rm had}}$	0.16	0.19	0.24	0.28	0.30	0.31	
$\frac{E_{\mu_1}-E_{\mu_2}}{E_{\mu_1}+E_{\mu_2}}$	0.49	0.46	0.41	0.39	0.37	0.41	

[a] From Ref. 5.

[b] The angle between the two muons in a plane perpendicular to the beam direction.

can still give a soft missing-energy spectrum if multihadron semileptonic decays[38] are considered.

IV. RESULTS

We have calculated various distributions based on the model discussed in Sec. II for all principal (counter and bubble chamber) experiments. Both (anti) neutrino-induced $\mu\mu$ and μe events are considered, and appropriate experimental cuts and flux-averaging have been applied to our predictions, so that direct comparison with experimental data can be made. For definiteness, we shall present in this section various distributions for the CDHS neutrino experiment, which at present has higher statistics than any other experiments, and investigate their sensitivity to the quark-fragmentation-function parametrizations. Other results [for the FHPRW, CFR, BC (Brookhaven-Columbia), and the BFHWW (Berkeley-Fermilab-Hawaii-Washington-Wisconsin, E546 at Fermilab) experiments] are available on request.

A. The CDHS experiment

We discuss here briefly the experimental setup and cuts imposed on the CDHS dimuon data. The CDHS experiment uses a combined function target and detector consisting of iron calorimeters and plastic scintillators for the detection of hadron showers, and toroidal magnets and drift chambers which measure the muon trajectories. A narrow-band beam (NBB) of neutrinos (antineutrinos), formed in the decay of momentum-selected (200 $\pm$14 GeV/c) hadrons, was used in their first attempt to look for dimuon events. The uncertainty in the neutrino energy is $\pm$20%.

The experimental cut imposed, which corresponds to a minimum range requirement, is

$$E_\mu > 4.5 \text{ GeV}.$$

This cut is most severe for the secondary muon, which tends to be quite soft.

B. Comparison with model predictions

The calculated right-sign muon energy spectrum is shown in Fig. 5. We find that it is not sensitively dependent on the choice of quark fragmentation functions, as can be anticipated, and fits the CDHS data rather well. The secondary muon spectrum, Fig. 6, in conrast, shows rather drastic variations: The high-energy end becomes more and more enhanced when we go from $(1/z)(1-z)$ to $z\ (1+z)$. When compared with data, we find that forms such as $(1/z)(1-z)$ and e^{-3z} fail to reproduce the data above 30 GeV, while the constant fragmentation function and others emphasizing large z values are able to give a more energetic spectrum and a slightly better fit to the data at the high-energy end. Notice that there is a substantial number of events in the first

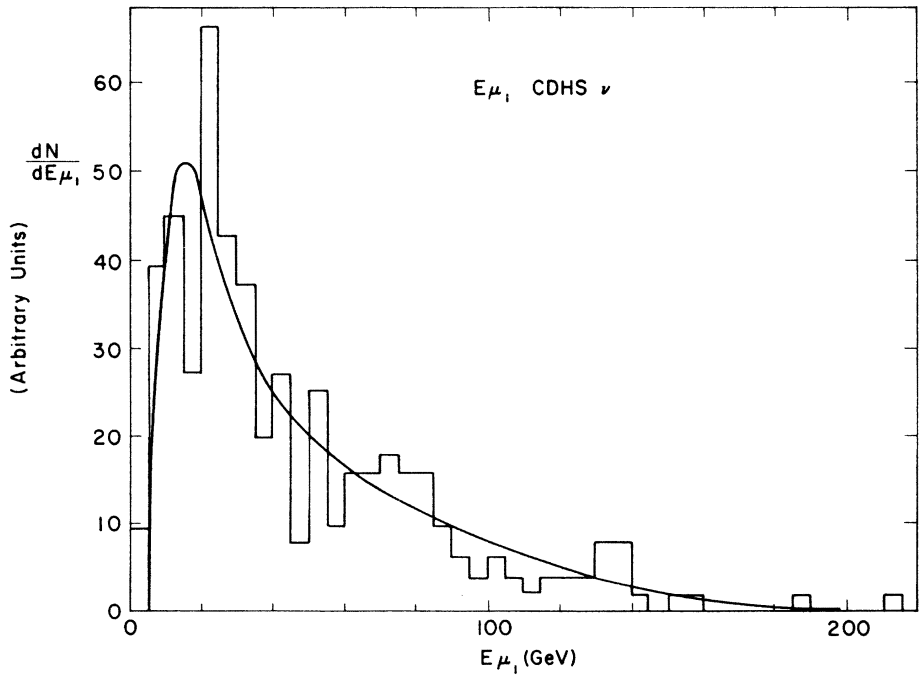

FIG. 5. Calculated leading-muon energy spectrum compared with the CDHS neutrino data.

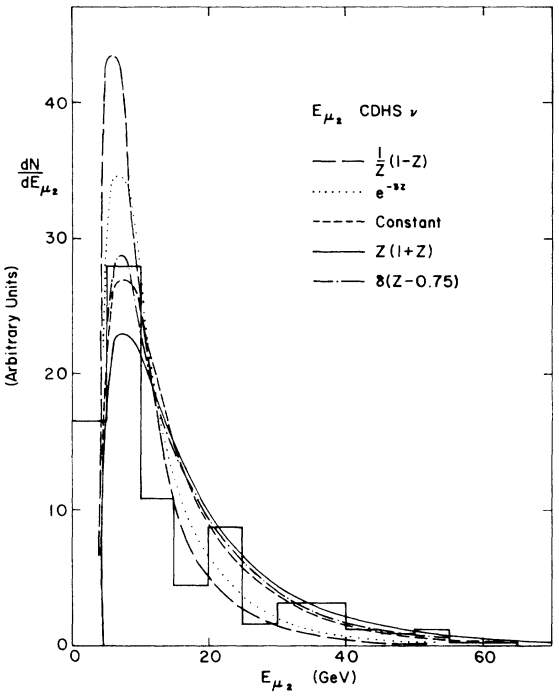

FIG. 6. Secondary-muon energy spectrum. The CDHS neutrino data are shown.

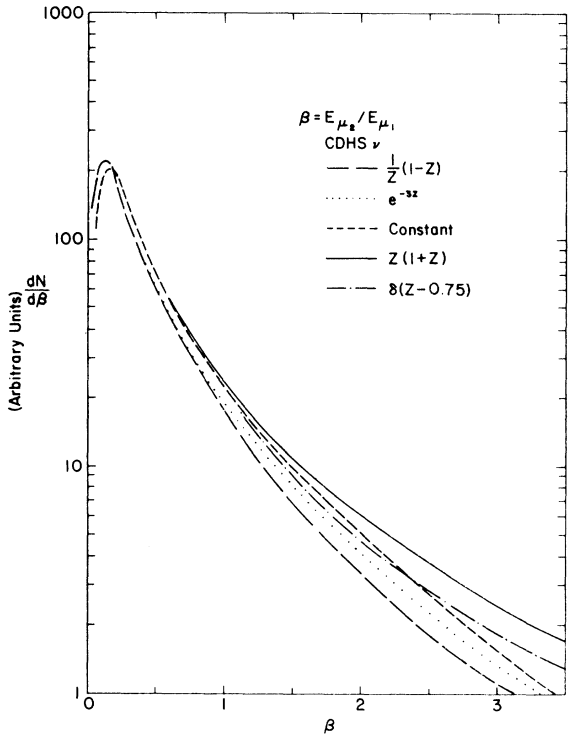

FIG. 7. Predicted distributions of the muonic energy ratio, $\beta = E_{\mu_2}/E_{\mu_1}$.

data bin (actually between ~4.5 and 5.0 GeV due to the energy cut), and the constant form as well as the $z(1+z)$ and $\delta(z-0.75)$ forms tend to underestimate the peak around 8.0 GeV. (This would become more apparent if the data were plotted, starting at 4 or 4.5 GeV, in 5-GeV bins.) We do not know to what extent the transverse-momentum spread in the quark fragmentation process will modify the distribution: Presumably a softer spectrum will result. This seems to indicate that the charmed-quark fragmentation function may indeed have a constant or slightly rising behavior as z goes to 1, as suggested by Odorico and Roberto,[39] but the present data on the secondary-muon energy spectrum will not be precise enough to establish this conclusively. The $z_{\mu_2} \equiv E_{\mu_2}/(E_{\mu_2}+E_{\mathrm{Had}})$ distribution may be a better place to look for the differentiation. This will be discussed below.

The interesting feature of a pronounced asymmetry between the energies of the two muons in these dimuon events is reproduced in our model calculations. In Fig. 7, the distributions of $\beta \equiv E_{\mu_2}/E_{\mu_1}$ are shown. For all choices of the fragmentation functions, a rather sharp peak is observed at ~0.2. Note that the value of β is unbounded above. A related variable reflecting the same asymmetry is $\gamma \equiv (E_{\mu_1}-E_{\mu_2})/(E_{\mu_1}+E_{\mu_2})$ and the distributions calculated using the various

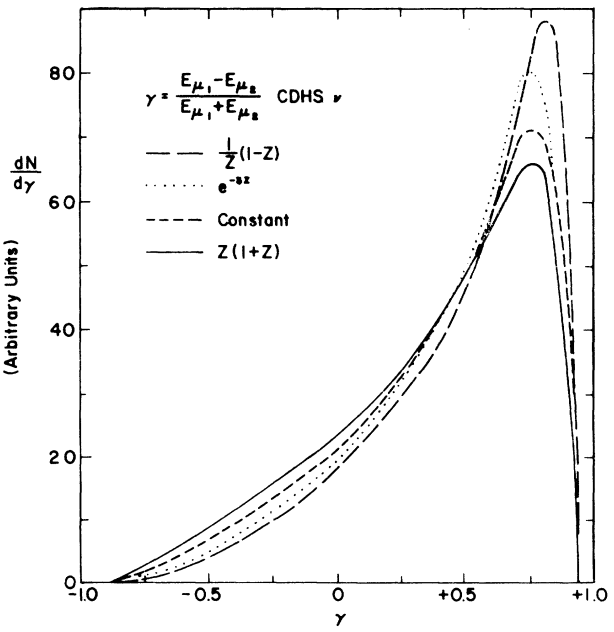

FIG. 8. Predicted distributions of the muonic energy asymmetry, $\gamma = (E_{\mu_1}-E_{\mu_2})/(E_{\mu_1}+E_{\mu_2})$.

fragmentation functions are shown in Fig. 8. The asymmetry in γ, favoring large positive γ values, is maintained even for fragmentation functions with substantial large z contributions, although a definite increase in the number of event for $\gamma < 0.5$ and negative γ values is evident. It should perhaps be noted that the population in the symmetric region $(-0.3 < \gamma < +0.3$, corresponding to $\frac{1}{2} < E_{\mu_1}/E_{\mu_2} < 2)$, although dependent on the choice of the fragmentation functions, is nonetheless substantial, ranging from ~22% for $(1/z)(1-z)$ to ~28% for $z(1+z)$. The muon energies correlation plots (Fig. 9) show this explicitly.

Next we consider the angular properties of the muons. In Figs. 10 and 11 are shown the dis-

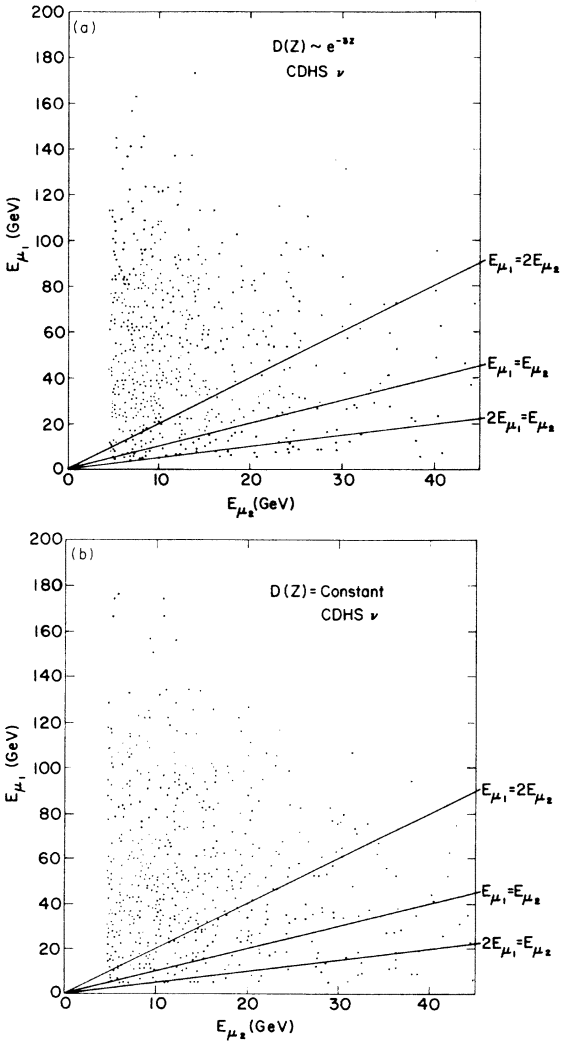

FIG. 9. (a) Muon-energies correlation plot for $D(z) \sim e^{-3z}$, normalized to approximately 500 events. (b) Muon-energies correlation plot for $D(z) =$ constant, normalized to approximately 500 events.

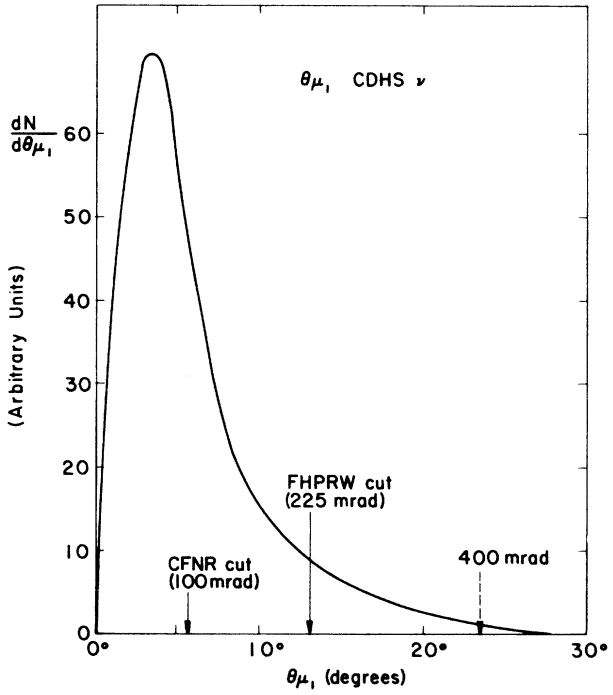

FIG. 10. Angular distribution in θ_{μ_1}.

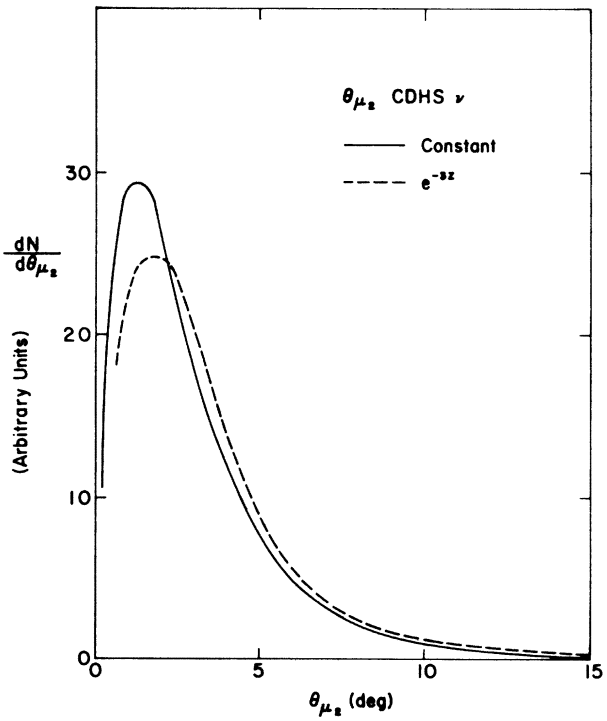

FIG. 11. Angular distributions in θ_{μ_2}.

tributions in θ_{μ_1} and θ_{μ_2}, where θ_μ is the angle between the muon momentum and the incident beam direction. We see that while the primary muon tends to emerge with small θ_μ, some experimental angular cuts can be quite severe. The CDHS experiment has very good acceptance up to ~400 mrad, whereas the FHPRW ($\theta_{\mu_1} < 225$ mrad for their old data) and CFR ($\theta_{\mu_1} < 100$ mrad) experiments generally lose a bulk of the events with $E_{\mu_1} > 4.5$ GeV. As is evident from Fig. 11, secondary muons surviving the energy cut also tend to stay close to the beam direction, and the effect of the high-z emphasis of the fragmentation function is to shift the peak towards smaller values. The angular cut turns out not to be of much significance. Figure 12 displays the distribution of $\theta_{\mu_2,\mathrm{Had}}$, the angle between the second muon and the hadron jet; the near collinearity between the muon and hadron-jet momenta is a reflection of the hadronic origin of the secondary muon. This also implies that in a plane perpendicular to the beam direction, the two muons tend to emerge (almost) back to back. The distribution in $\Delta\phi$, Fig. 13, shows this explicitly: A large amount of events are observed at large $\Delta\phi$. The sharp peaking at 180° in our theoretical predictions may be somewhat smoothed out when the transverse-momentum spread in the quark fragmentation process is included, since some of this transverse momentum

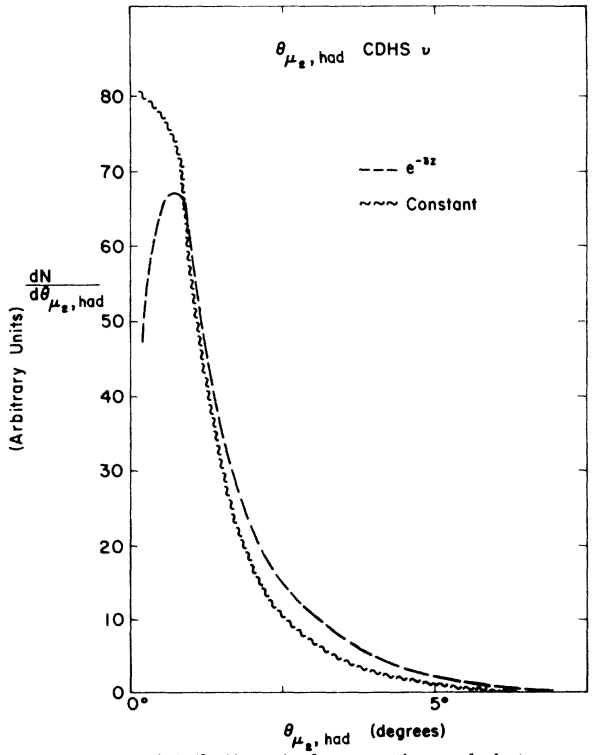

FIG. 12. Distributions in $\theta_{\mu_2,\mathrm{had}}$, the angle between the secondary muon and the hadron-shower momenta.

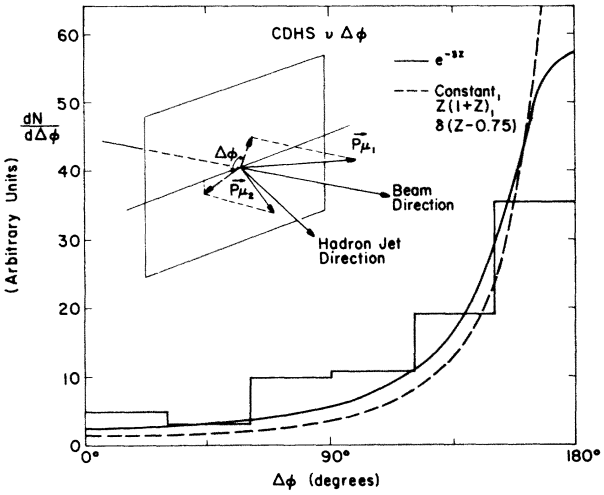

FIG. 13. Distributions of the azimuthal angle between the two muons; the CDHS data are plotted.

will be passed on to the second muon. In any case, the large $\Delta\phi$ peak of the data is reproduced.

The dimuon invariant-mass $M_{\mu\mu}$ distributions are given in Fig. 14. One characteristic of the distributions is the tailing off at larger values of $M_{\mu\mu}$, but extending beyond 9 GeV/c^2, due to the different origins of the two muons. This is to be contrasted with the cases where the dimuons come from a heavy-lepton decay ($L^0 \to \mu^-\mu^+\nu$) or two-body decay of a hadron ($H \to \mu^+\mu^-$), where the $M_{\mu\mu}$ distribution would cut off at the mass of L^0 or H. The theoretical curves with $(1/z)(1-z)$ and e^{-3z} are able to reproduce the peak at ~2 GeV/c^2, but miss the high-mass end (only slightly for e^{-3z}). The other forms of fragmentation functions give broader distributions, though consistently underestimate the low-mass peak.

Next we turn to the scaling variables x and y. We first note that an intrinsic characteristic of our model calculation is that an unobserved neutrino necessarily carries away some energy. Figure 15(a) shows the "missing-energy" spectrum. The effect of the choice of the quark fragmentation function is fairly obvious: The spectrum has a longer high-energy tail for fragmentation functions with substantial large-z contributions. This in turn will directly affect the total visible energy spectrum ($E_{\mathrm{vis}} \equiv E_{\mu_1} + E_{\mu_2} + E_{\mathrm{Had}}$), shown in Fig. 15(b). The first peak in the spectrum, essentially those events induced by pion neutrinos, is more or less fixed for all fragmentation functions, due to the fact that at these relatively low energies, the missing neutrino is constrained to be rather soft by the cut on the muon energies. At higher energies, events

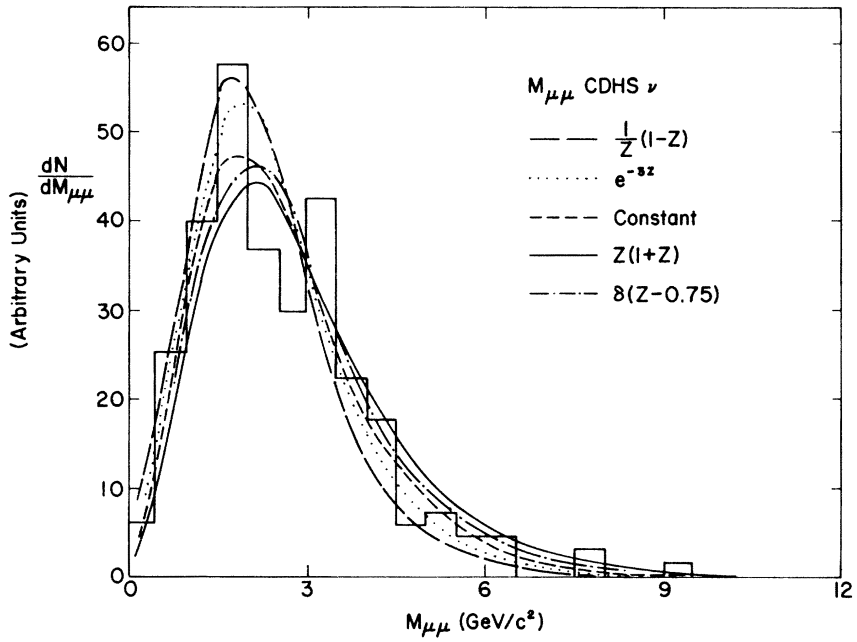

FIG. 14. Dimuon invariant-mass distributions. The CDHS data are displayed.

with energetic missing neutrinos can indeed occur quite frequently, and the second peak of kaon neutrino events shifts progressively towards smaller visible energies and broadens considerably. Experimentally then, we expect

$$E_{\rm vis} \leq E\,,$$

$$x_{\rm vis} = \frac{E_{\mu_1} E_{\rm vis}(1-\cos\theta_{\mu_1})}{m_N(E_{\rm vis}-E_{\mu_1})} \geq x\,,$$

$$y_{\rm vis} = (E_{\rm vis}-E_{\mu_1})/E_{\rm vis} \leq y\,.$$

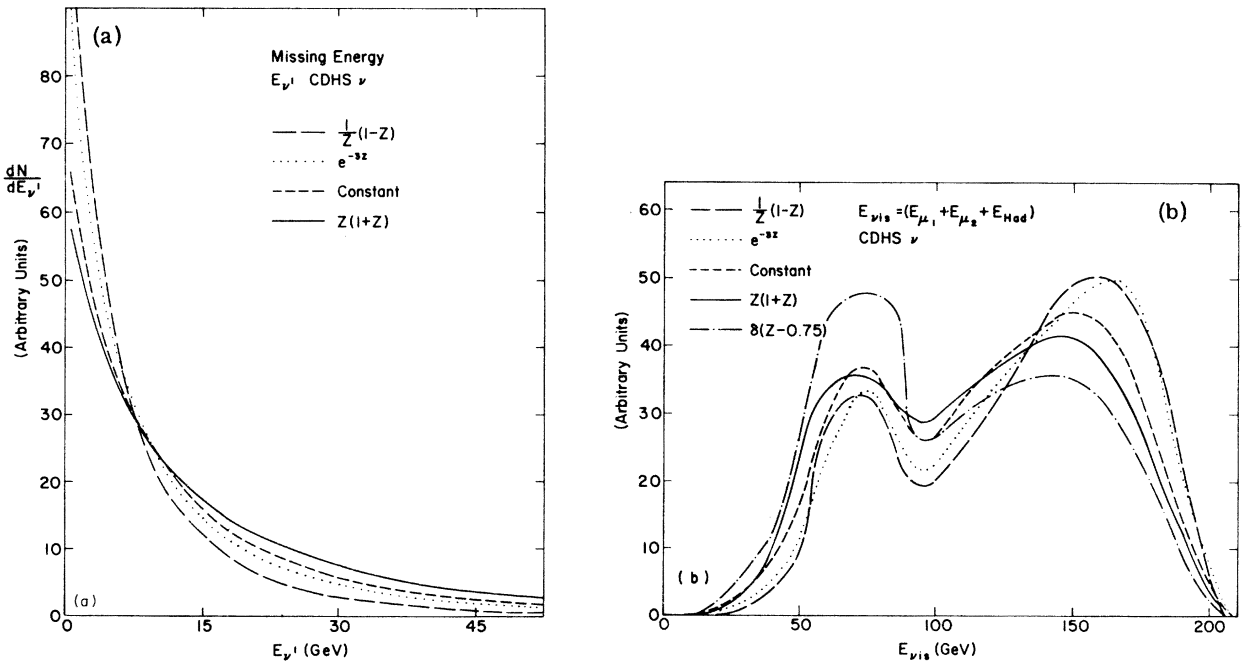

FIG. 15. (a) The missing-energy spectra for different fragmentation functions. (b) Visible-energy distributions.

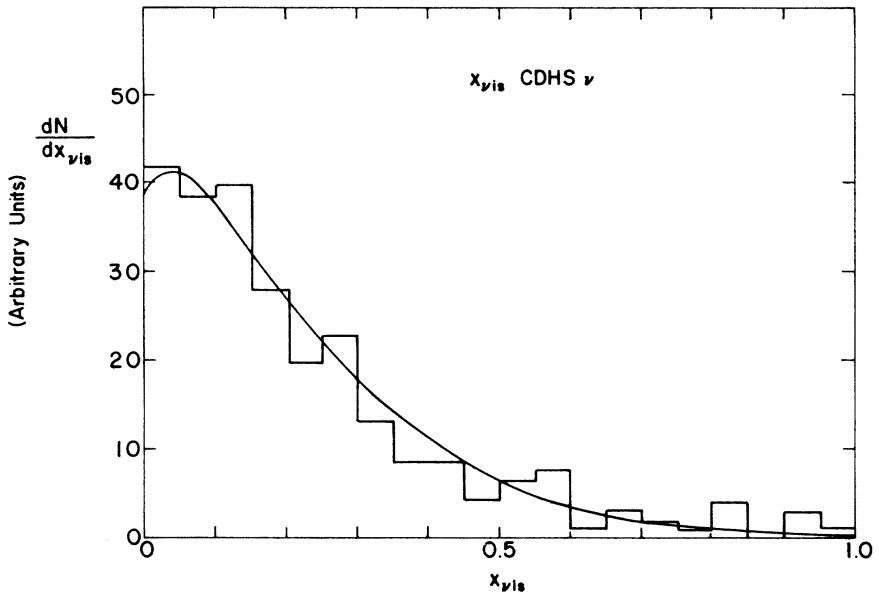

FIG. 16. The x_{vis} distribution. The CDHS data are plotted.

The calculated distributions for x_{vis} and y_{vis} are shown in Figs. 16 and 17. The effect of the choice of quark fragmentation functions does not quite show up in the x_{vis} distribution, and an excellent agreement with data is obtained. For the y_{vis} distribution, there seems to be an excess of events for $y_{vis} < 0.3$ in the CDHS data which cannot be accounted for even by fragmentation functions with large-z emphasis. The $z(1+z)$ and $\delta(z-0.75)$ forms in particular also fail to reproduce the peak at large y_{vis}, where the $(1/z)(1-z)$, e^{-3z} and constant forms seem to give a fair fit to the data.

We mentioned earlier that in diffractive production of charm, little energy is imparted to the nuclear target, and observed hadrons, just as the secondary muons, obtain their energy from the

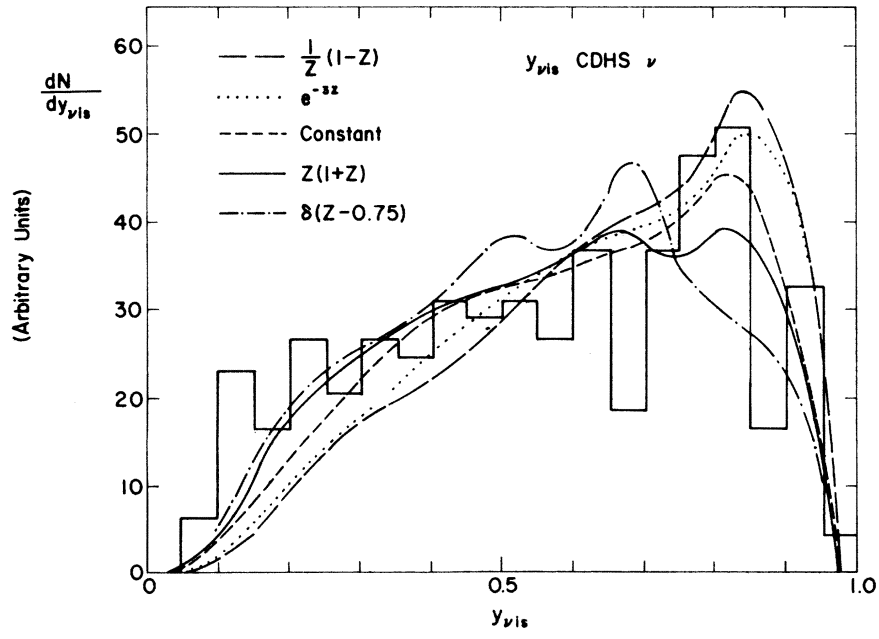

FIG. 16.

FIG. 17. The v_{vis} distributions. The CDHS data are plotted.

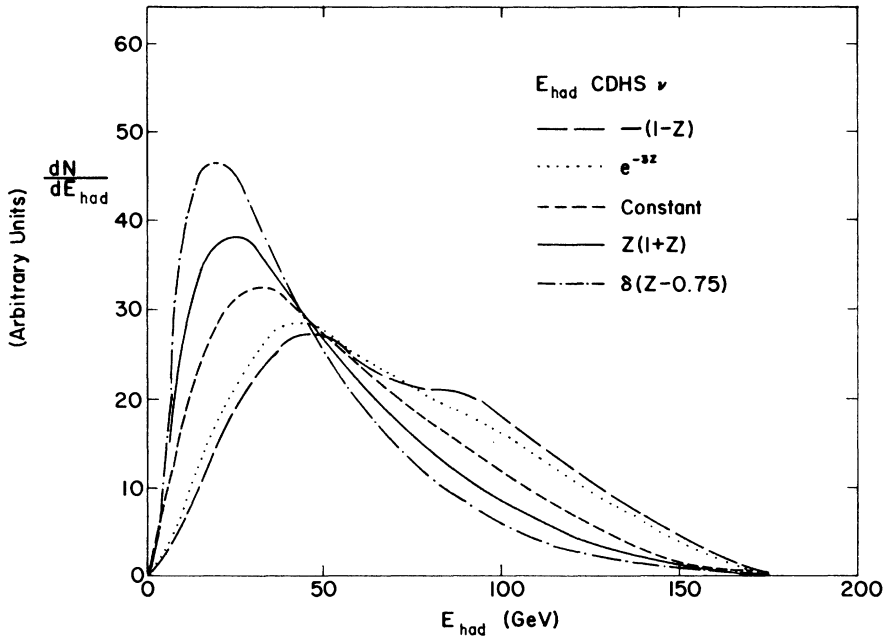

FIG. 18. The hadronic-energy distributions.

semileptonic decay of C^*. In contrast, the hadronic energy spectrum in our deep-inelastic case receive contributions from two main sources: In the fragmentation process as well as the semileptonic decay of the charmed hadron. The hadronic energy distribution from the semileptonic decay can be expected to resemble that of the secondary muon, peaking at small values; whereas the hadronic energy from the fragmentation process obviously depends on the choice of the fragmentation function. Our theoretical predictions for the overall hadronic energy distribution are shown in Fig. 18. These are generally broad and extending close to the maximum energy of ~200 GeV. With the charmed hadron getting a large portion of the energy transfer in the case with $D(z)$ emphasizing large-z values, the E_{Had} distribution shifts correspondingly towards lower energies.

It is pointed out by Odorico[22] that another useful variable for the determination of the correct form of $D(z)$ is

$$z_{\mu_2} = \frac{E_{\mu_2}}{E_{\mu_2} + E_{\mathrm{had}}} .$$

In Fig. 19, we display the distributions of z_{μ_2} for the various choices of $D(z)$—the sensitivity to the form of the fragmentation function to some extent can be anticipated from our earlier discussion on the secondary muon and hadronic energy distribution. We must add that the value of z_{μ_2}, for $D(z) = \delta(z - z_0)$ is bounded above by z_0, since the charmed hadrons never get more than z_0 of the total energy transfer.

Before concluding, we mention briefly here our results for antineutrino interactions. Very similar distributions are obtained which are in reasonable agreement with the data. In particular, there is no evidence for any right-handed coupling of the form $(u, b)_R$, which would introduce a val-

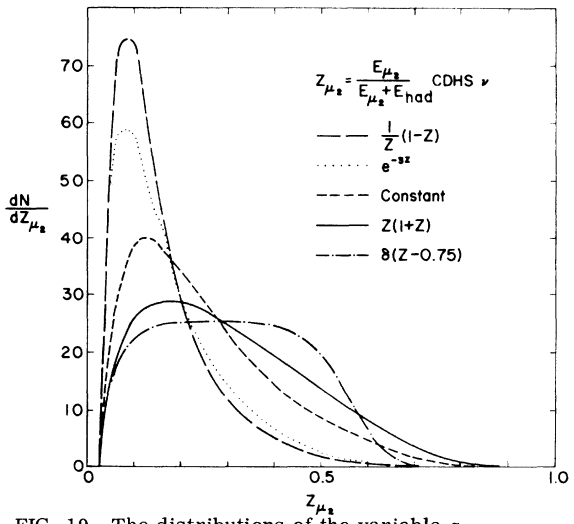

FIG. 19. The distributions of the variable $z_{\mu_2} = E_{\mu_2}/(E_{\mu_2} + E_{Had})$.

ence-quark component to the x distribution, and, because of the higher threshold, a shift toward large values in the y distribution. Because of the limited statistics, differentiation between the different quark fragmentation functions is much less conclusive.

V. CONCLUDING REMARKS

In this work, we have considered deep-inelastic opposite-sign dimuon production by neutrinos within the context of the GIM-Weinberg-Salam model, and compared the predictions directly with the CDHS neutrino data by applying the appropriate cuts and flux-averaging. The theoretical assumptions on the form of the charmed-quark fragmentation function have been examined. From this study we can draw several conclusions.

First, the uncertainty in the choice of fragmentation function aside, the neutrino dimuon data are well described by our calculations, except for the $y_{\rm vis}$ distribution where an excess of events are observed at low $y_{\rm vis}$. There is also no indication from the comparison of our predictions with data of any evidence for the need to introduce right-handed interactions or new quarks.

Second, the observed $\sigma^{\nu}(\mu^-\mu^+)/\sigma^{\nu}(\mu^-)$ ratio and its energy dependence require a fragmentation function with some contribution from the high-z region e^{-3z} and constant $D(z)$ are preferred candidates, although other forms of the fragmentation function cannot be excluded decisively in view of the uncertainty in the semileptonic branching ratio. The calculated average values of various experimental observables, when compared with data, also seem to indicate a preference for the forms e^{-3z} and constant.

We do not find complete systematic agreement between the calculated distributions and available data with any one of the fragmentation functions considered in this study. Of all the quantities that directly reflect the choice of the fragmentation functions, the z_{μ_2} distribution appears to be the most sensitive test. The secondary-muon energy spectrum has a high-energy tail that seems to favor the constant, $z(1+z)$, or even $\delta(z-0.75)$ forms, while the low-energy peak in the data is better described by forms favoring small z values. A similar pattern is observed in the comparison of theoretical predictions with data for the dimuon invariant-mass distribution: Here again the $(1/z)(1-z)$ and e^{-3z} forms reproduce the low-mass peak, but fail in the high-mass region, where constant, and $z(1+z)$ seem to fair better. The $y_{\rm vis}$ distribution quite definitely rules out the $\delta(z-0.75)$ form, and if further data confirms the peak at $y_{\rm vis}\sim 0.8$, then the $z(1+z)$ form will also be ruled out. The $(1/z)(1-z)$, e^{-3z} and constant forms, though they describe the data reasonably well at large $y_{\rm vis}$, all fall below the data for $y_{\rm vis}<0.3$.

Except for the $y_{\rm vis}$ distribution, the results of the present study seem to suggest that the charmed-quark fragmentation function (in the present range of energy transfers) is likely to have a behavior that, while peaking at small-z values (e.g., like e^{-3z}), has nonetheless substantial (constant?) values at large z. Apart from waiting for higher statistics on the dimuon events, the experimental data on neutrino induced μ^-e^+ events, with a smaller cut on the positron energy, may provide further information on the charmed-quark fragmentation function, particularly at small-z values. We may also look into the inclusive lepton spectra in e^+e^- annihilations (where the charmed quarks will have well-defined energies) for an improvement in our understanding of the charmed-quark fragmentation process. In addition, hadronic decays of charmed hadrons, observable in e^+e^- annihilations and neutrino interactions in bubble chambers, should also be an important source of information.

ACKNOWLEDGMENTS

I am particularly grateful to C. Quigg for suggesting this investigation and for his constant guidance and encouragement. Many of the numerical techniques used in this study were learned from C.H. Albright and D. Carey, and I have benefitted from discussions with C.H. Albright, J.D. Bjorken, R.E. Shrock, and J. Smith. I would also like to thank C. Quigg, C.H. Albright and J. Smith for reading the manuscript.

---

*Submitted to the Department of Physics, The University of Chicago, in partial fulfillment of the requirements for the Ph.D. degree.

†Operated by Universities Research Association Inc. under contract with the Energy Research and Development Administration.

[1]A. Benvenuti *et al.*, Phys. Rev. Lett. 34, 419 (1975); 35, 1199 (1975); 1203 (1975); 35, 1249 (1975).

[2]B. C. Barish *et al.*, Phys. Rev. Lett. 36, 939 (1976); 39, 981 (1977).

[3]C. Baltay *et al.*, Phys. Rev. Lett. 35, 1249 (1975); 35, 1199 (1975); 39, 62 (1972); P. Bosetti *et al.*, *ibid.* 38,

1248 (1977).
[4]J. Blietschau *et al.*, Phys. Lett. 60B, 207 (1976).
[5]M. Holder *et al.*, Phys. Lett. 69B, 377 (1977); R. Turlay, talk given at the International Conference on Neutrino Astrophysics, Elbrus, U. S. S. R., 1977 (unpublished).
[6]See, for example, L. M. Sehgal and P. M. Zerwas, Nucl. Phys. B108, 483 (1976); E. Derman, *ibid.* B110, 40 (1976); L. N. Chang and J. N. Ng, Phys. Rev. D 16, 3157 (1977).
[7]B. Aubert *et al.*, Phys. Rev. Lett. 33, 984 (1974); A. Benvenuti *et al.*, *ibid.* 36, 1478 (1976).
[8]A. Benvenuti *et al.*, Phys. Rev. Lett. 37, 189 (1976).
[9]A. De Rújula, H. Georgi, S. L. Glashow, and H. R. Quinn, Rev. Mod. Phys. 46, 391 (1974); R. M. Barnett, Phys. Rev. Lett. 36, 1163 (1976); Phys. Rev. D 14, 70 (1976); C. H. Albright and R. E. Shrock, Phys. Rev. D 16, 575 (1977).
[10]M. Holder *et al.*, Phys. Rev. Lett. 39, 433 (1977); R. Turlay, talk given at the International Conference on Neutrino Physics and Neutrino Astrophysics, Elbrus U. S. S. R., 1977 (unpublished) J. Steinberger, lectures at the Cargese Summer Institute, 1977 (unpublished).
[11]B. C. Barish *et al.*, Phys. Rev. Lett. 39, 1595 (1977); 39, 981 (1977).
[12]P. C. Bosetti *et al.*, Phys. Lett. 70B, 273 (1978).
[13]F. A. Nezrick, invited talk at the Triangle Seminar on Recent Developments in High Energy Physics, Campione D'Italia, 1977, Fermilab Report No. FERMILAB-Conf-77/112-EXP (unpublished).
[14]H. Georgi and H. D. Politzer, Phys. Rev. Lett. 36, 1281 (1976); Phys. Rev. D 14, 1826 (1976); A. De Rújula, H. Georgi, and H. D. Politzer, Phys. Rev. D 15, 2495 (1977), and references therein.
[15]S. L. Glashow, J. Iliopoulos, and L. Maiani, Phys. Rev. D. 2, 1285 (1970).
[16]S. Weinberg, Phys. Rev. Lett. 19, 1264 (1967); A. Salam, in *Elementary Particle Theory*, edited by N. Svartholm (Almqvist and Wiksell, Stockholm, 1962), p. 367.
[17]M. B. Einhorn and B. W. Lee, Phys. Rev. D 13, 43 (1976); M. K. Gaillard, S. A. Jackson, and D. V. Nanopoulos, Nucl. Phys. B102, 326 (1976); L. N. Chang, E. Derman, and J. N. Ng, Phys. Rev. Lett. 35, 1252 (1975).
[18]F. Bletzacker and H. T. Nieh, SUNY–Stony Brook Report No. ITP-SB-77-42, 1977 (unpublished).
[19]M. Holder *et al.*, Phys. Lett. 70B, 396 (1977).
[20]H. Goldberg, Phys. Rev. Lett. 39, 1598 (1977).
[21]See, e.g., S. L. Adler, Report No. NAL-CONF-74/39-THY (unpublished); or L. M. Sehgal, Argonne Report No. ANL/HEP/PR75-45 (unpublished).
[22]C. G. Callan and D. J. Gross, Phys. Rev. Lett. 22, 156 (1969).
[23]R. P. Feynman, *Photon-Hadron Interactions* (Benjamin, New York, 1972); M. Gronau, F. Ravndal, and Y. Zarmi, Nucl. Phys. B51, 611 (1973).
[24]E. Derman, Nucl. Phys. B110, 40 (1976); R. Odorico, Phys. Lett. 71B, 121 (1977).
[25]R. D. Field and R. P. Feynman, Phys. Rev. D 15, 2590 (1977).
[26]S. Pakvasa, D. Parashar, and S. F. Tuan, Phys. Rev. D 10, 2124 (1974).
[27]D. W. Duke and F. E. Taylor, Phys. Rev. D 17, 1788 (1978).
[28]F. T. Dao *et al.*, Phys. Rev. Lett. 39, 1388 (1977).
[29]D. M. Kaplan *et al.*, Phys. Rev. Lett. 40, 435 (1978).
[30]A. Seiden, Phys. Lett. 68B, 157 (1977).
[31]V. Barger, T. Gottschalk, and R. J. N. Phillips, Phys. Lett. 70B, 51 (1977).
[32]M. Gronau, C. H. Llewellyn Smith, T. Walsh, S. Wolfram, and T. C. Yang, Nucl. Phys. B123, 47 (1977).
[33]M. Suzuki, Phys. Lett. 71B, 139 (1977).
[34]J. D. Bjorken, Phys. Rev. D 17, 171 (1978).
[35]V. N. Gribov and L. N. Lipatov, Phys. Lett. 37B, 78 (1971); Yad. Fiz. 15, 1218 (1972) [Sov. J. Nucl. Phys. 15, 675 (1972)]; 15, 781 (1972) [15, 438 (1972)]; Y. Eylon and Y. Zarmi, Nucl. Phys. B83, 475 (1974).
[36]V. G. Kartvelishvili *et al.*, ITEP report, 1977 (unpublished), and references therein.
[37]R. M. Barnett and F. Martin, Phys. Rev. D 16, 2765 (1977).
[38]V. Barger *et al.*, Phys. Rev. D 16, 746 (1977).
[39]R. Odorico and V. Roberto, Nucl. Phys. B136, 333 (1978).

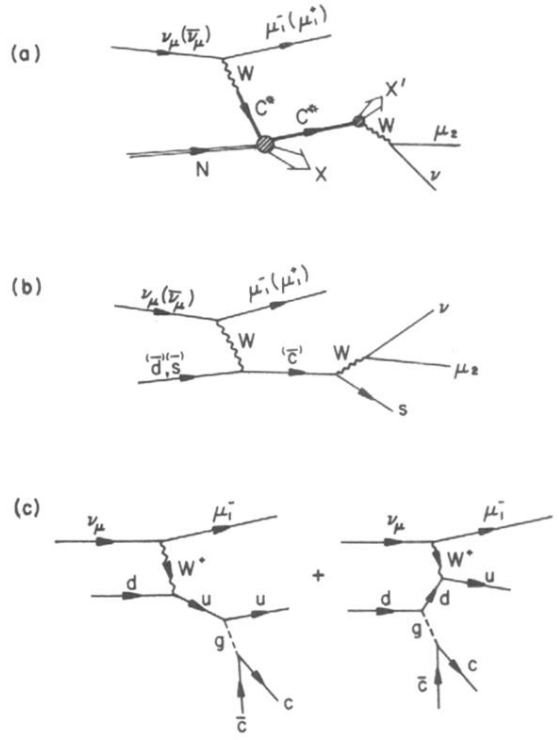

FIG. 1. (a) Diffractive production of a charmed vector meson C^* and subsequent semileptonic decay. (b) Light-quark-to-charmed-quark transition and subsequent $c \to s\mu\nu$ decay. (c) Neutrino-induced associated production of charm in QCD. The dotted lines denote colored gluons.

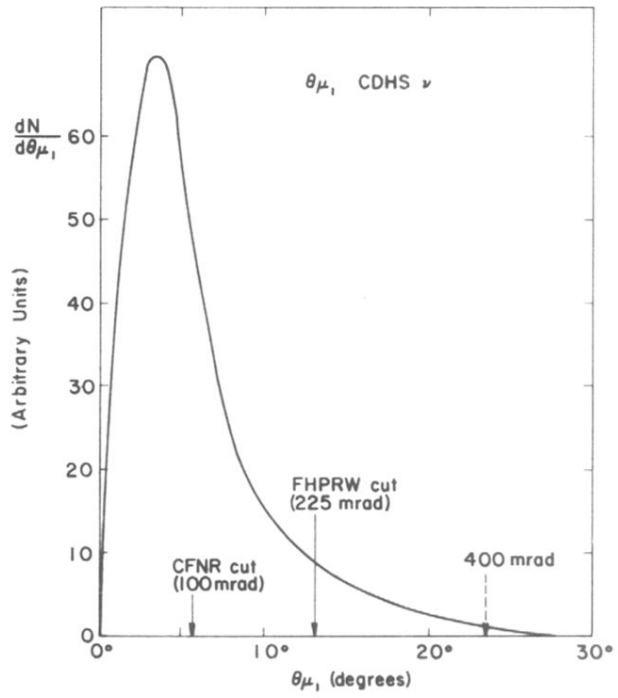

FIG. 10. Angular distribution in θ_{μ_1}.

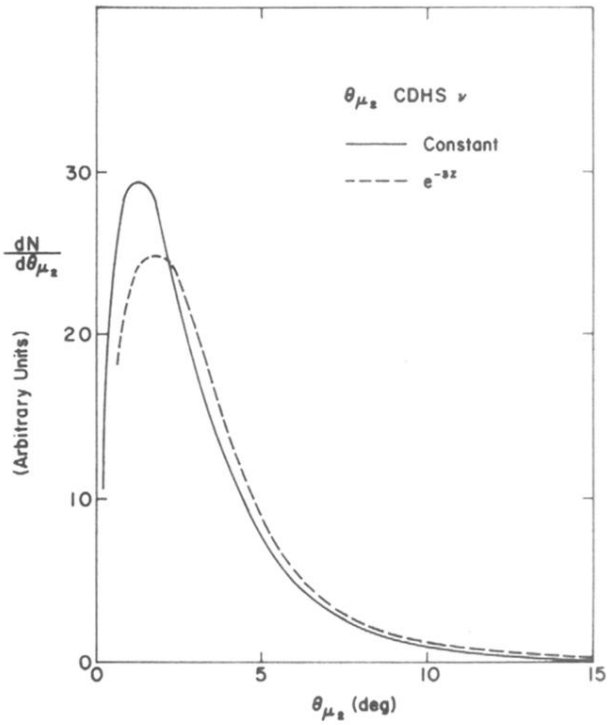

FIG. 11. Angular distributions in θ_{μ_2}.

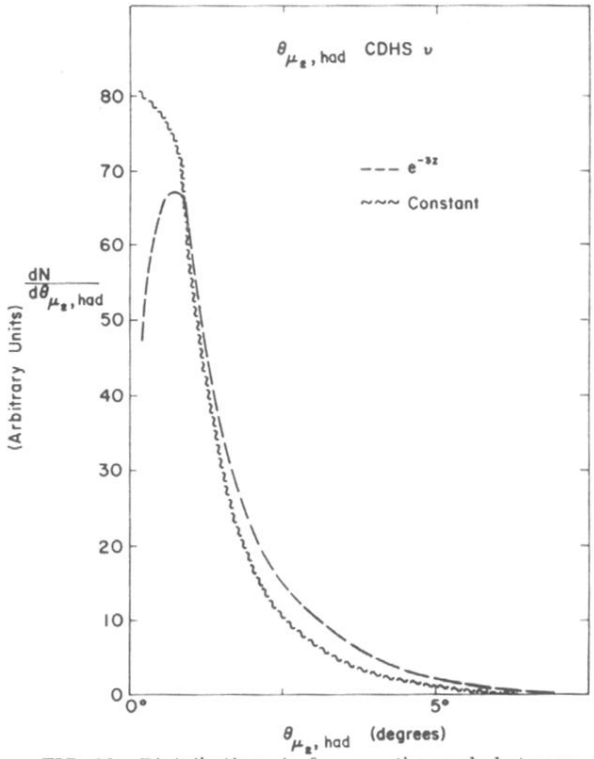

FIG. 12. Distributions in $\theta_{\mu_2, had}$, the angle between the secondary muon and the hadron-shower momenta.

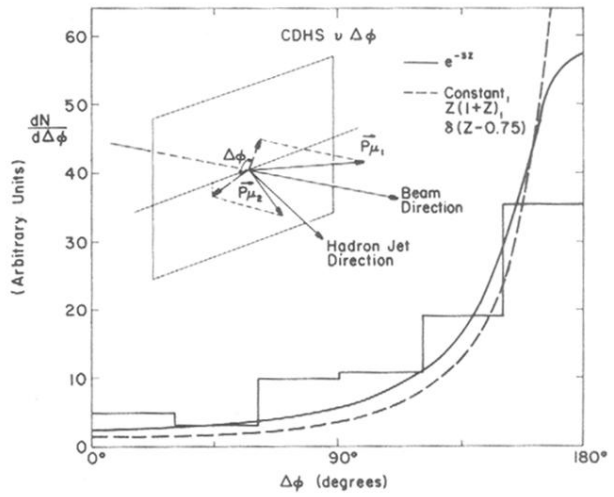

FIG. 13. Distributions of the azimuthal angle between the two muons; the CDHS data are plotted.

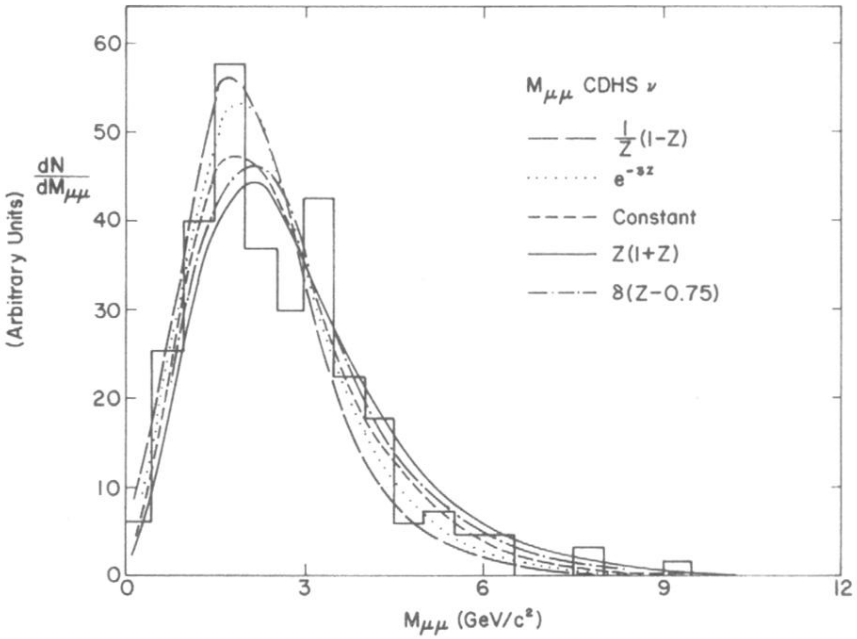

FIG. 14. Dimuon invariant-mass distributions. The CDHS data are displayed.

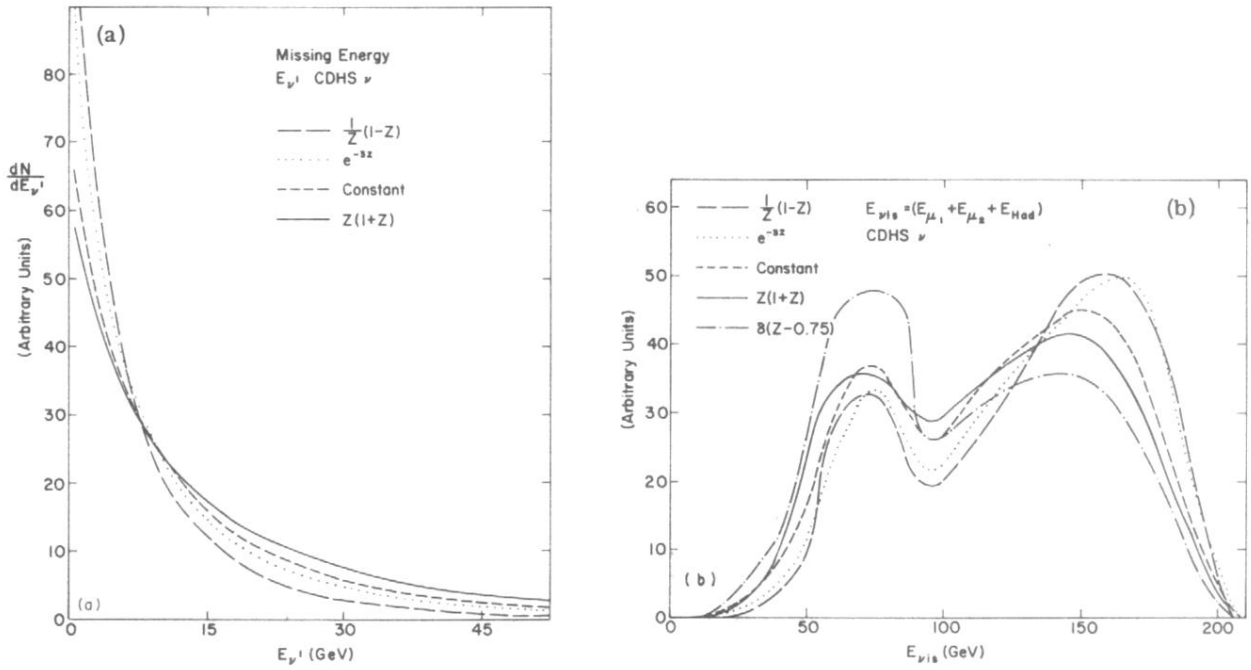

FIG. 15. (a) The missing-energy spectra for different fragmentation functions. (b) Visible-energy distributions.

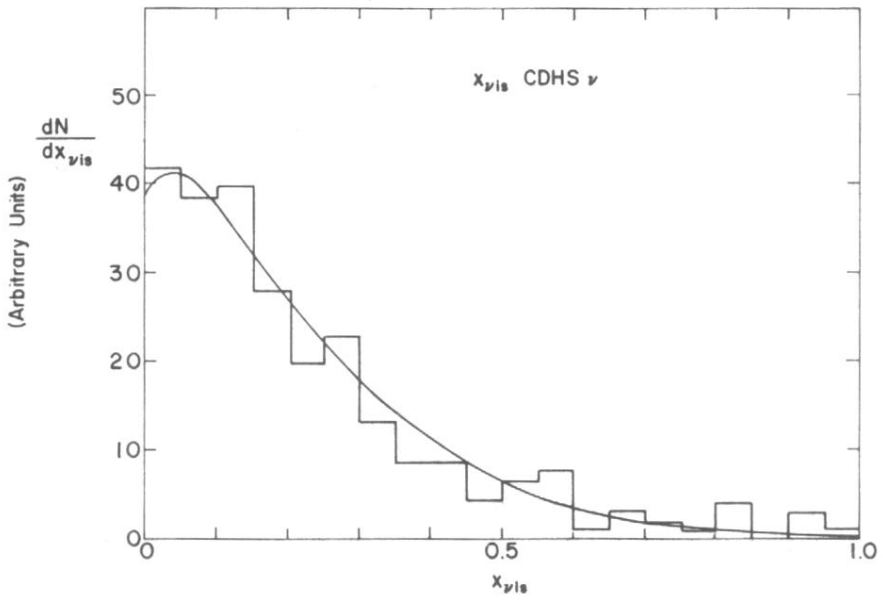

FIG. 16. The x_{vis} distribution. The CDHS data are plotted.

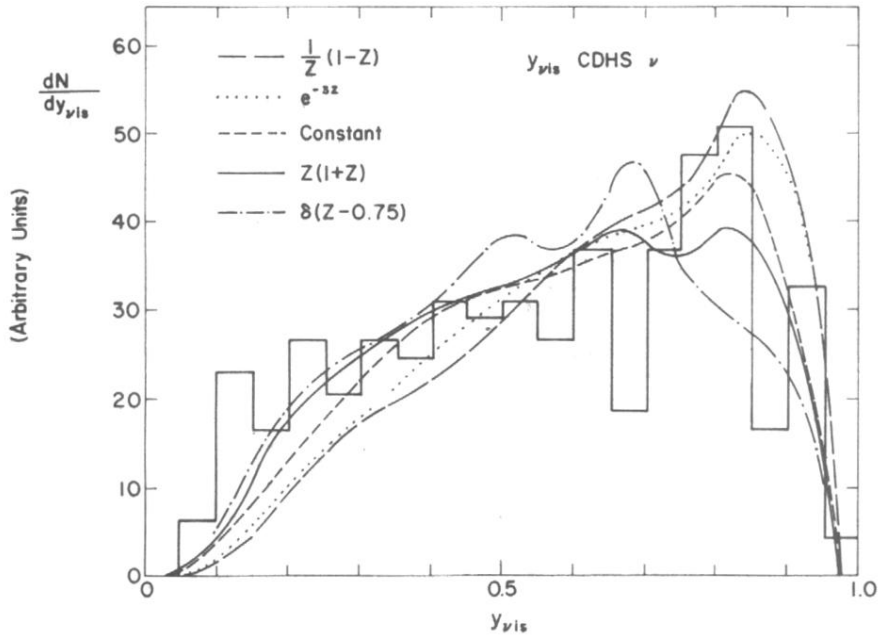

FIG. 17. The y_{vis} distributions. The CDHS data are plotted.

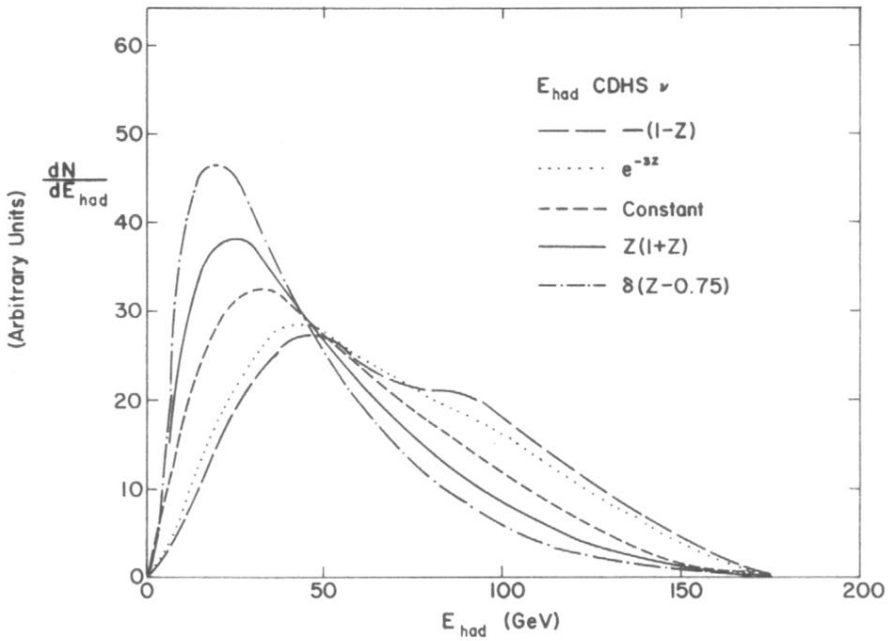

FIG. 18. The hadronic-energy distributions.

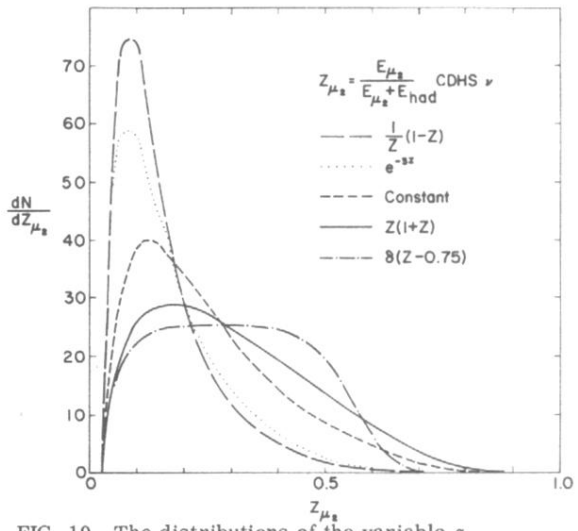

FIG. 19. The distributions of the variable $z_{\mu_2} = E_{\mu_2}/(E_{\mu_2} + E_{Had})$.

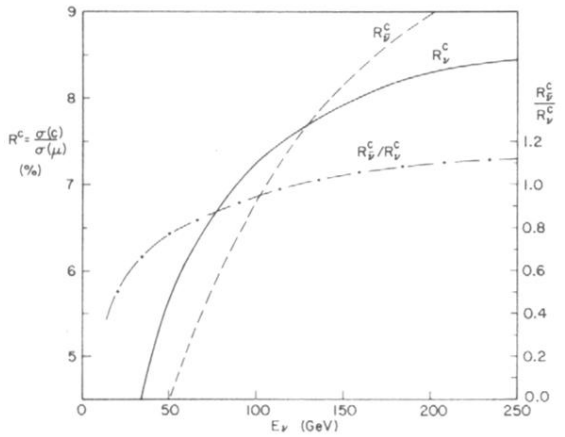

FIG. 2. Charm-production cross section, relative to single-muon charged-current (noncharm) cross section, as a function of incident neutrino energy.

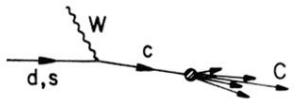

FIG. 3. Charmed-quark fragmentation into a charmed hadron C and other physical hadrons.

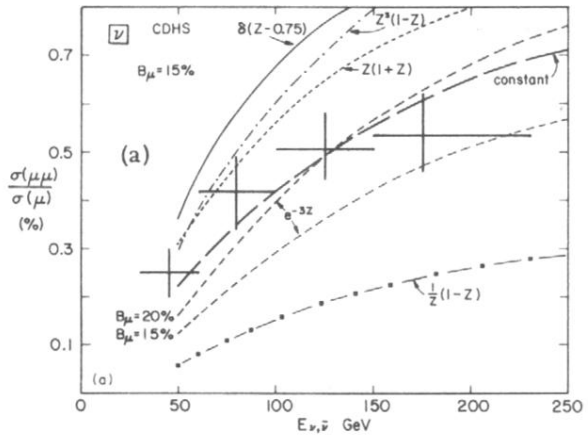

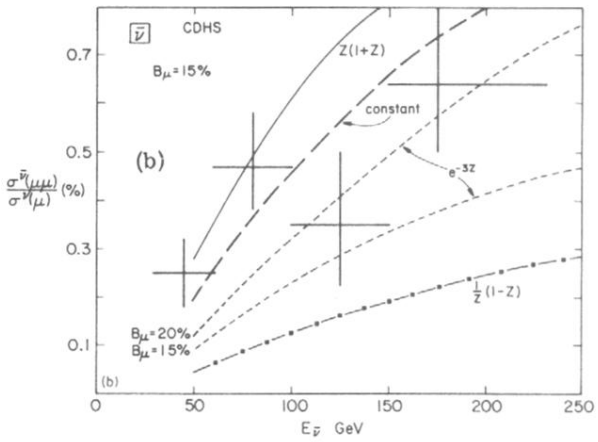

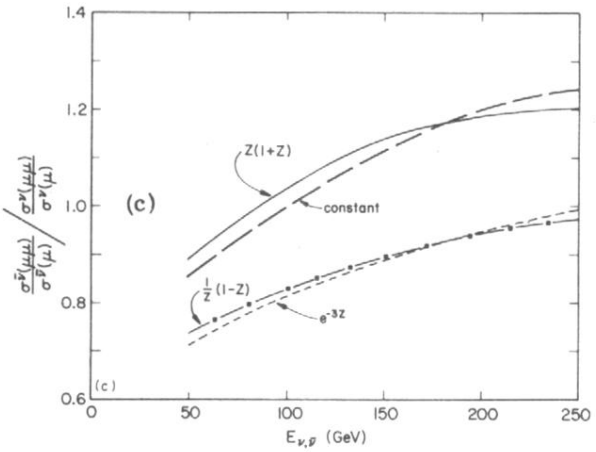

FIG. 4. (a) Energy dependence of the cross-section ratio $\sigma^{\nu}(\mu\,\mu)/\sigma^{\nu}(\mu)$. The CDHS muon energy cuts are applied. (b) Energy dependence of the cross-section ratio $\sigma^{\bar{\nu}}(\mu\,\mu)/\sigma^{\bar{\nu}}(\mu)$. The CDHS muon energy cuts are applied. (c) The ratio of dimuon production ratios as a function of (anti)neutrino energy. The CDHS muon energy cuts are applied.

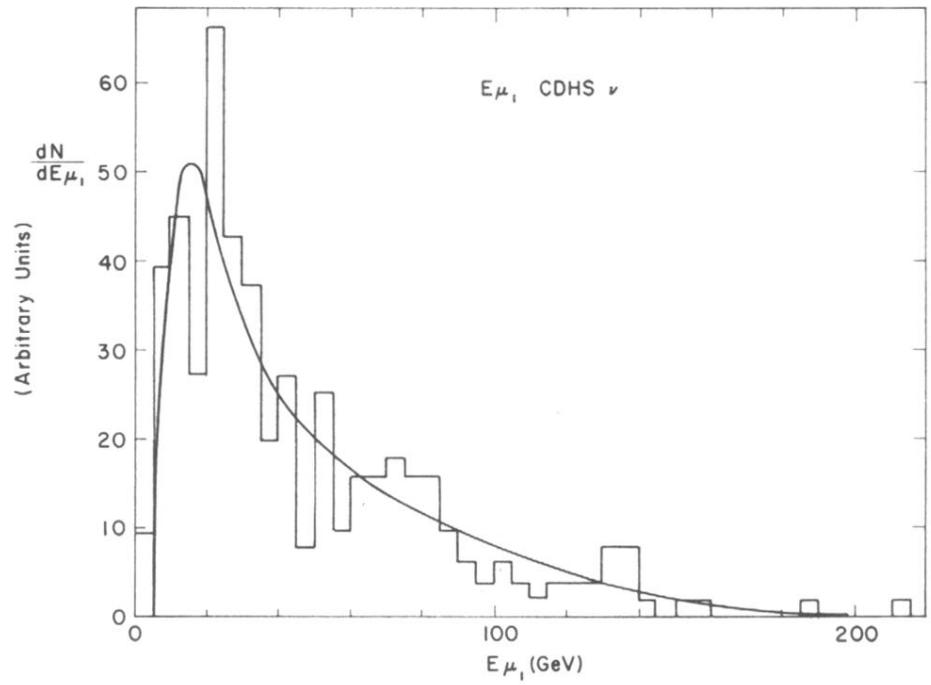

FIG. 5. Calculated leading-muon energy spectrum compared with the CDHS neutrino data.

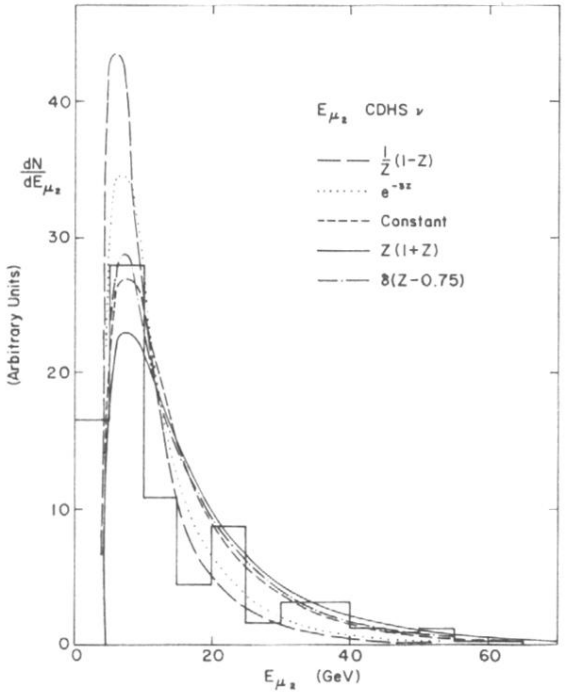

FIG. 6. Secondary-muon energy spectrum. The CDHS neutrino data are shown.

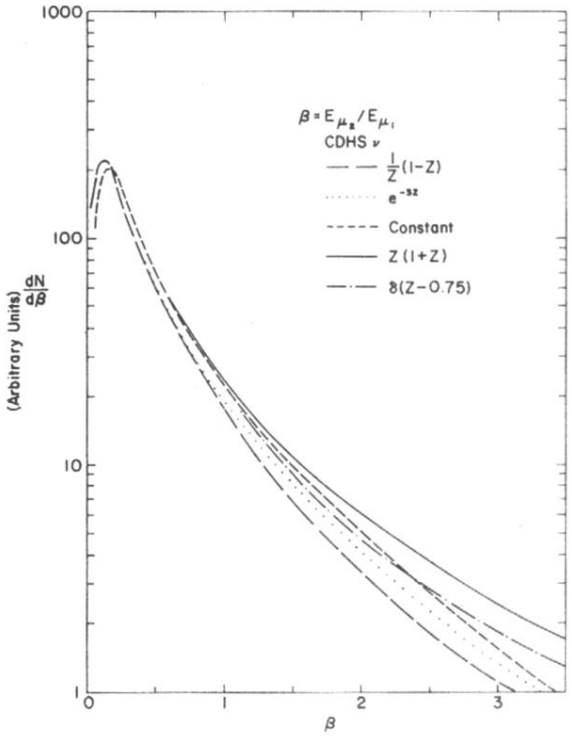

FIG. 7. Predicted distributions of the muonic energy ratio, $\beta = E_{\mu_2}/E_{\mu_1}$.

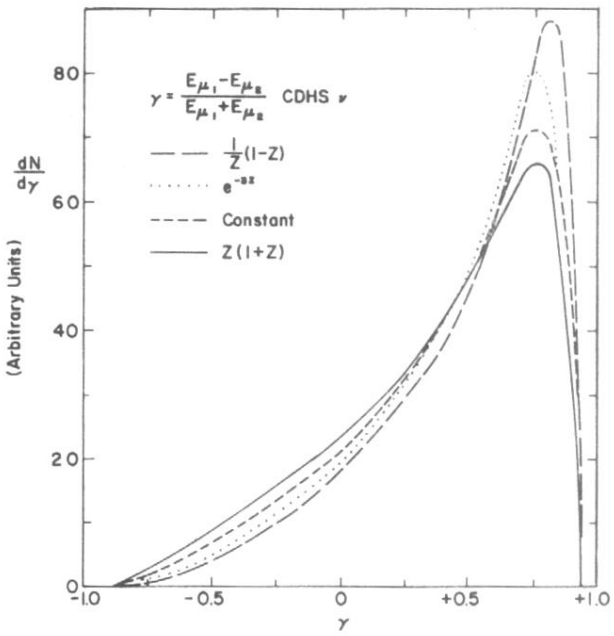

FIG. 8. Predicted distributions of the muonic energy asymmetry, $\gamma = (E_{\mu_1} - E_{\mu_2})/(E_{\mu_1} + E_{\mu_2})$.

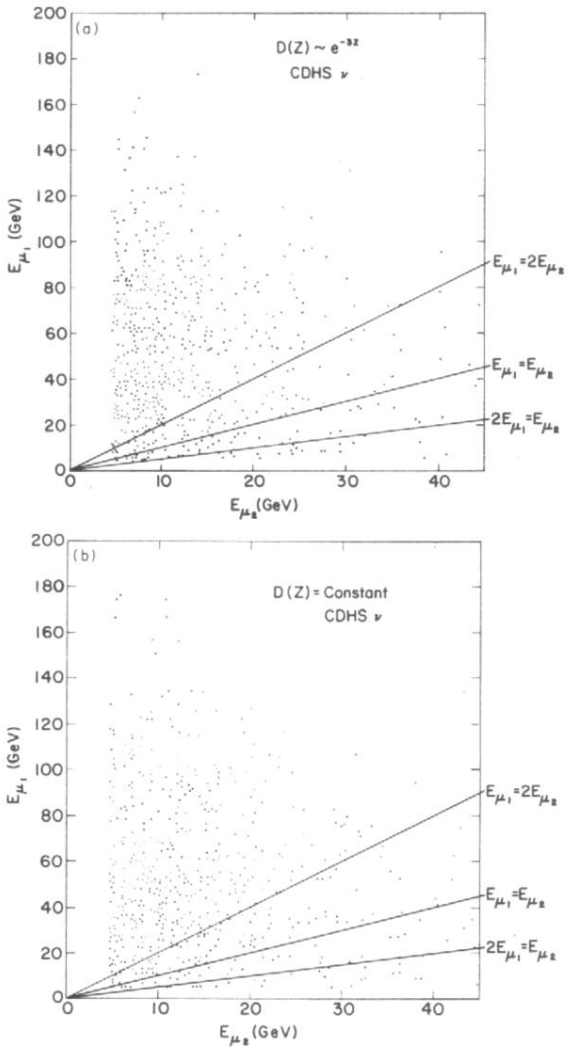

FIG. 9. (a) Muon-energies correlation plot for $D(z) \sim e^{-3z}$, normalized to approximately 500 events. (b) Muon-energies correlation plot for $D(z) = \text{constant}$, normalized to approximately 500 events.